DANMARKS OG GRØNLANDS
GEOLOGISKE UNDERSØGELSE
RAPPORT 1996/51

Energy Research Project No. 1323/91-0012 and 1323/93-0018 Combustion Char Characterisation

Final Report

By Per Rosenberg, Henrik Ingermann Petersen, Henning Sund Sørensen, Erik Thomsen and Carsten Guvad

GEUS

DANMARKS OG GRØNLANDS
GEOLOGISKE UNDERSØGELSE
RAPPORT 1996/51

Energy Research Project No. 1323/91-0012 and 1323/93-0018 Combustion Char Characterisation

Final Report

By Per Rosenberg, Henrik Ingermann Petersen, Henning Sund Sørensen, Erik Thomsen and Carsten Guvad

GEUS
Geological Survey of
Denmark and Greenland

1 INDEX

2 INTRODUCTION

In 1991 funding was granted to the Geological Survey of Denmark and Greenland, GEUS, (the former Geological Survey of Denmark) as a continuation of the research activities in the field of coal characterisation in relation to combustion properties.

The scope of the project was to correlate reactivity measures of raw coals and the maceral concentrates of the coals obtained in a previous project (Thomsen, 1993) with the morphology of the chars produced in the same project, using a heated wire grid devolatilisation method. In a phase 2 of the project, the results should be incorporated in a three dimensional boiler model, performed by The Technical University of Denmark, The Laboratory of Heating and Air Conditioning.

Numerous problems arose during the project. First of all, the chars from the heated wire grid were not comparable with combustion chars produced by other workers in the field. The chars were not fused and comprised the original coal texture, and additionally the particles were too small to allow a classification. Consequently it was decided to use chars produced in an earlier Energy Research Project (Thomsen et al., 1993). One group of chars were produced in a Drop Tube reactor at Studsvik at relatively low-temperatures and heating rates, and another group of chars were produced in a Laminar Flow Reactor at Sandia National Laboratories at heating rates and temperatures similar to the conditions in a p.f. combustion boiler.

The results from the two set of chars lacked consistency in texture, i.e. chars produced from the same coal in the two reactors were not comparable.

Due to the late stage in the project period it became obvious that the data could not be incorporated in the 3 D modelling, first of all it was not clear which chars were representative of the "real world" chars and further the numbers of coals involved were too limited. Therefore it was decided to delete the 3 D modelling from the project and in lieu continue the morphology/porosity study involving chars produced at full scale experiments at Fynsværket (Laursen and Larsen, 1995) together with chars produced in various reactors at Research Centre Risø.

The work involves determination of morphology, "macroporosity" and a detailed study in Scanning Electron Microscope. The latter is issued as a separate Combustion Char Atlas (Sørensen and Rosenberg, 1996), together with a CD ROM with all the images in TIFF format, enabling the user to study the texture in full resolution on a PC.

3 REACTOR TYPES

The chars studied in this project are produced in a great variety of reactors, spanning from simple experimental set-ups, such as the muffle furnace, to much more complex and sophisticated reactors such as the Sandia Laminar Flow Reactor and the Risø Tunnel reactor, both capable of operating at temperatures and heating rates very close to full scale conditions. Together with these chars, also chars produced in full scale experiments at Fynsværket were included.

In Table 3.1 the various reactors are listed together with the typical test conditions. Chars were produced at heating rates and under temperature and oxygen conditions close to full scale conditions in a 1.5 MW tunnel reactor (1.5MW) at Research Centre RISØ, (Jensen et al. ,1992), in a Laminar Flow Reactor (LFR) at the Sandia National Laboratories, (Hardesty et al., 1978, Mitchell et al., 1992 and Jensen and Mitchell., 1993), and in an Entrained Flow reactor (EFR) at Research Centre RISØ (Sørensen et al., 1991), and under conditions very far from realistic pulverised fuel (p.f.) combustion in the Drop Tube Furnace (DTF) at Studsvik Energy AB (Jensen and Thomsen, 1990). At the low extreme were the Muffle Furnace (MF) experiments at Research Centre Risø (Sørensen, 1994), where chars were produced at very low heating rates and with a final temperature not exceeding 900 °C.

Chars produced at a heated wire grid, (Thomsen, 1993), were originally included in the project, but for the reasons already mentioned in chapter 2, these were excluded.

The chars from the DTF and the LFR are chars produced during an earlier Energy Research Project and were thus in stock. Chars from the MF, 1.5 MW and the EFR were kindly made available by Dr. L. H. Sørensen at Research Centre Risø. The chars from the full scale experiments at Fynsværket were sampled by K. Laursen, GEUS during her Ph.D. study of fouling and slagging tendencies of coals.

Thus the sample set represent the most common techniques used to obtain and study the char reactivity in the laboratory environments together with full scale chars, which have proved to be invaluable for the purpose of establishing a reference for "real life p.f. combustion chars".

Reactor type	Experimental conditions
Full Scale Fynsværket block 07	Temperature ca. 1500 °C Particle size: ca. 70 μm 410 MW tangential fired p.f. boiler. Burmeister & Wain 4AF-LN, low NO_x burner. Full load, 3% oxygen in flue gas.
1.5 MW tunnel reactor	Temperature ca. 1300-1400 °C 4% oxygen in flue gas Particle size: 97% < 90 μm IFRF block swirl burner Tunnel p.f. combustor
Laminar Flow Reactor	Temperature: c. 1400 °C Heating rate 10^4-10^5 K/s Oxygen: 6 and 12 mole-% Wall temperature ca. 500 K Particle size: 106-125 μm
Entrained Flow Reactor	Temperature 1330 °C Heating rate 10^5 K/s 3% oxygen Particle size: 75-135 μm
Drop Tube Furnace	Temperatures: 800, 1000 and 1150 °C Atmospheric air Particle size: 106-125 μm
Muffle Furnace	Temperature 900 °C Heating rate 1000 °C/min Atmospheric air Particle size: 106-125 μm.

Table 3.1 List of reactors used for char production together with the typical test conditions.

4 COAL TYPES AND DERIVED COMBUSTION CHARS

4.1 Coal types

The number of different coals used in this study is rather limited. The reason is that only few coals are studied both under low temperature and under high temperature conditions. The coal types used for the char production are listed in Table 4.1.

The mean random reflectance of the Colombian coal (Co) and the two Australian coals (Au1 and Au2) indicates a high volatile bituminous C rank. The two South African coals (SA1 and SA2) have higher mean random reflectances and are of high volatile bituminous A and B rank, respectively.

The Colombian coal has the highest vitrinite content and the lowest inertinite content of the five coals. In contrast the four Gondwana coals are dominated by inertinite, in particular the South African coals, which contain only 20 vol. % vitrinite. The Polish coal is probably a mixture of two single coal types. More detailed petrographic information is given in chapter 7.

Petrography	**Coal sample composition(vol. %)**					
	Co	**Au1**	**Au2**	**SA1**	**SA2**	**Po**
Vitrinite	75	27	37	20	20	54
Liptinite	6	3	7	3	6	5
Inertinite	17	69	54	75	72	28
Vitrinite Reflectance (mean random Ro)						
	0.59	0.62	0.63	0.80	0.71	0.74/1.03

Table 4.1 Coal types, their maceral group composition and their rank.

4.2 Char sampling plan

Legend	Reactor Type	Burnout(daf) %	Sample position	Temperature
CoA	Muffle Furnace	33	-	900 °C
CoB	Drop tube	12	290mm(215 ms)	800 °C
CoC	Drop tube	32	490 mm(363 ms)	800 °C
CoD	Drop tube	53	610 mm(452 ms)	800 °C
CoE	Drop tube	64	740 mm(548 ms)	800 °C
CoF	Drop tube	32	290 mm(215 ms)	1000 °C
CoG	Drop tube	66	490 mm(363 ms)	1000 °C
CoH	Drop tube	27	140 mm(104 ms)	1150 °C
CoI	Drop tube	54	290 mm(215 ms)	1150 °C
CoJ	Laminar Flow Reactor	61	64 mm(47 ms)	1682 K(6% O2)
CoT*	Laminar Flow Reactor	62	129 mm(72 ms)	1642 K(6% O2)
CoK	Laminar Flow Reactor	66	191 mm(95 ms)	1593 K(6% O2)
CoL	Laminar Flow Reactor	69	254 mm(117 ms)	1536 K(6% O2)
CoM	Laminar Flow Reactor	59	64 mm(47 ms)	1692 K(12% O2)
CoN	Laminar Flow Reactor	70	129 mm(72 ms)	1645 K(12% O2)
CoU*	Laminar Flow Reactor	79	191 mm(95 ms)	1591 K(12% O2)
CoV*	Laminar Flow Reactor	84	254 mm(117 ms)	1532 K(12% O2)
CoO	Full Scale	25	Flame zone	ca. 1500 °C
CoP	Full Scale	63	Flame zone	ca. 1500 °C
CoQ	Full Scale	79	Flame zone	ca. 1500 °C
CoR	1.5 MW tunnel reactor	50	-	ca. 13-1400 °C
CoS	Entrained Flow reactor	52	250 ms	1330 °C
Au1A	Muffle Furnace	24	-	900 °C
Au1B	Drop tube	28	290 mm(215 ms)	800 °C
Au1C	Drop tube	68	490 mm(363 ms)	800 °C
Au1D	Drop tube	76	740 mm(548 ms)	800 °C
Au1E	Drop tube	10	140 mm(104 ms)	1000 °C
Au1F	Drop tube	55	290 mm(215 ms)	1000 °C
Au1G	Drop tube	89	490 mm(363 ms)	1000 °C
Au1H	Drop tube	86	290 mm(215 ms)	1150 °C
Au1I	Laminar Flow Reactor	42	64 mm(47 ms)	1682 K(6% O2)
Au1J	Laminar Flow Reactor	49	129 mm(72 ms)	1642 K(6% O2)
Au1K	Laminar Flow Reactor	52	191 mm(95 ms)	1593 K(6% O2)
Au1L	Laminar Flow Reactor	56	254 mm(117 ms)	1536 K(6% O2)
Au1M	Laminar Flow Reactor	46	64 mm(47 ms)	1692 K(12% O2)
Au1N	Laminar Flow Reactor	58	129 mm(72 ms)	1645 K(12% O2)
Au1O	Laminar Flow Reactor	66	191 mm(95 ms)	1591 K(12% O2)
Au1P	Laminar Flow Reactor	72	254 mm(117 ms)	1532 K(12% O2)
Au2A	Muffle Furnace	28	-	900 °C
Au2B	Drop tube	46	290 mm(215 ms)	800 °C
Au2C	Drop tube	62	490 mm(363 ms)	800 °C
Au2D	Drop tube	75	610 mm(452 ms)	800 °C
Au2E	Drop tube	51	140 mm(104 ms)	1000 °C
Au2F	Drop tube	76	290 mm(215 ms)	1000 °C
Au2G	Drop tube	91	490 mm(363 ms)	1000 °C
Au2H	Drop tube	98	740 mm(548 ms)	1000 °C
Au2I	Drop tube	87	290 mm(215 ms)	1150 °C
Au2J	Drop tube	97	390 mm(289 ms)	1150 °C
Au2K	Laminar Flow Reactor	49	64 mm(47 ms)	1682 K(6% O2)

Legend	Reactor Type	Burnout(daf) %	Sample position	Temperature
Au2L	Laminar Flow Reactor	54	129 mm(72 ms)	1642 K(6% O2)
Au2M	Laminar Flow Reactor	58	191 mm(95 ms)	1593 K(6% O2)
Au2N	Laminar Flow Reactor	61	254 mm(117 ms)	1536 K(6% O2)
Au2O	Laminar Flow Reactor	49	64 mm(47 ms)	1692 K(12% O2)
Au2P	Laminar Flow Reactor	62	129 mm(72 ms)	1645 K(12% O2)
Au2Q	Laminar Flow Reactor	66	191 mm(95 ms)	1591 K(12% O2)
Au2R	Laminar Flow Reactor	71	254 mm(117 ms)	1532 K(12% O2)
SA1A	Full Scale	49	Flame zone	ca. 1500 °C
SA1B	Full Scale	73	Flame zone	ca. 1500 °C
SA1C	Full Scale	61	Flame zone	ca. 1500 °C
SA1D	Full Scale	71	Flame zone	ca. 1500 °C
SA2A	1.5 MW tunnel reactor	43	-	ca. 13-1400 °C
SA2B	Entrained Flow reactor	52	250 ms	1330 °C
PoA	Full Scale	63	Flame zone	ca. 1500 °C
PoB	Full Scale	65	Flame zone	ca. 1500 °C
PoC	Full Scale	61	Flame zone	ca. 1500 °C
PoD	Full Scale	-	Flame zone	ca. 1500 °C
*	The chars have been used only in the porosity and SEM study			

Table 4.2 List of chars used in the study, reactor types, burnout(daf), sample position together with the approximate temperature at the sampling position.

In Table 4.2 the total numbers of chars reported are listed. Although some experiments provided a great number of chars, a rather limited burnout interval is represented. Only the Colombian derived chars from the LFR represent burnout above 80%. The study focused on the burnout region at 50% to 60 %. The reason is that this burnout interval ensures that the chars are completely devolatilised and on the other hand not burned in a degree that would influence the morphology significantly.

The full scale chars were sampled by a suction pyrometer on a sintered 40 μm (nominal pore size) bronze filter. The drawback using a filter is that in the beginning of the sampling period the filter let small particles pass, but as the filter clock through time, the smaller particles are held back . In this way, the sampling method may be selective for certain inorganic particles, and thus the calculated burnout values for the full scale chars could be biased, and should only be used for information. For example the burnout of CoO (25%) is unrealistic and is contradicted by the morphology and the reflectance observed.

All burnout values are calculated using the ash tracer method.

Due to problems in polishing some of the samples , probably associated with the inorganic matrix, morphology measurements could not be performed on the three Colombian chars, CoT, CoU and CoV.

5 CHAR CLASSIFICATION

The char samples were embedded in epoxy resin, and polished blocks suited for reflected light microscopy were prepared. Char analyses were undertaken by point-counting 300 char particles in oil immersion in each sample.

The char classification system used in the present study follows mainly the guidelines outlined by Bailey et al. (1990), but it also incorporates the modifications suggested at the annual meeting of the International Committee for Coal and Organic Petrology (ICCP) in Chania, Crete, in 1993. It is based on the identification of seven char morphotypes or groups (tenuisphere, tenuinetwork, crassisphere, crassinetwork/mixed network/mixed, inertoid, fusinoid/solid, mineroid) and unburned coal particles. The different char morphotypes are identified on the basis of their morphology, char-wall thickness and porosity, as shown in Table 5.1.

The tenuisphere and crassisphere morphotypes are hollow spherical to angular chars with porosities above 80% and 60%, respectively. Additionally 75% of the wall area in tenuisphere chars should be <5 μm, whereas 75% of the wall area in crassisphere chars is >5 μm. Together with the tenuinetwork morphotype these two morphotypes constitute high-porosity chars. Tenuinetwork chars are characterised by an internal network structure, and 75% of the wall area is <5 μm. The porosity is above 70%.

A group of chars with intermediate porosities (40-70%) is united in the crassinetwork/mixed network/mixed morphotype group. The chars may show internal network structure with 75% of the wall area >5 μm or they may be composed of a fused and unfused part.

The inertoid and fusinoid/solid morphotypes are characterised by a low-porosity. Inertoid chars are dense with porosities between 5-40%, whereas the fusinoid/solid chars exhibit inherited cellular fusinite structure or are solid particles with porosities <5 %.

The mineroid morphotype is composed of mineral-rich chars (more than 50% mineral matter) with variable porosity. Together with unburned coal particles the morphotype is omitted from the correlations/calculations in the present study, and thus the remaining six morphotypes have been normalised to 100%. This is done to strengthen the correlations between the petrography of the parent coals and the resulting char morphotypes.

	Char type	Description
	Tenuisphere	Spherical to angular, porosity >80%, 75% of wall area <5 microns
	Crassisphere	Spherical to angular, porosity >60%, 75% of wall area >5 microns
	Tenuinetwork	Internal network structure, porosity >70%, 75% of wall area < 5 microns
	Crassinetwork/ Mixed network/ Mixed	Char with internal network structure with 75% of wall area > 5 microns or char with a fused and unfused part, porosity 40-70%
	Inertoid	Dense, porosity 5-40%, 75% of wall area > 5 microns
	Fusinoid/Solid	Inherited cellular fusinite structure or solid particle with < 5% porosity
	Mineroid	Particle with > 50% inorganic matter
	Coal	Particle of unburnt coal

Table 5.1 Char Classification after J. Bailey, ICCP Combustion Working Group Round Robin 1995.

6 CHAR MORPHOLOGY AND MACROPOROSITY CHARACTERISATION

6.1 Temperature influence on char morphology

Chars from the Colombian coal have been produced in all the reactors used in this study. This gives an excellent opportunity for a direct comparison of the influence of different experimental conditions on the formation of the char morphotypes, and further allows the comparison of the various laboratory derived char samples with full scale p.f. combustion char samples. The proportion of individual char morphotypes in each sample is shown in figure 6.1. A clear shift in composition between the low temperature DTF chars (CoB to CoI) and the high temperature chars (CoJ to CoS) is observed with respect to the tenuisphere, the crassisphere -morphotypes, and the mixed morphotype group. The three remaining morphotypes constitute a more random proportion of the samples. The low temperature DTF chars are more rich in the thin-walled morphotypes with high-porosity, whereas the high temperature chars are dominated by the thicker-walled crassisphere chars and the mixed morphotype group.

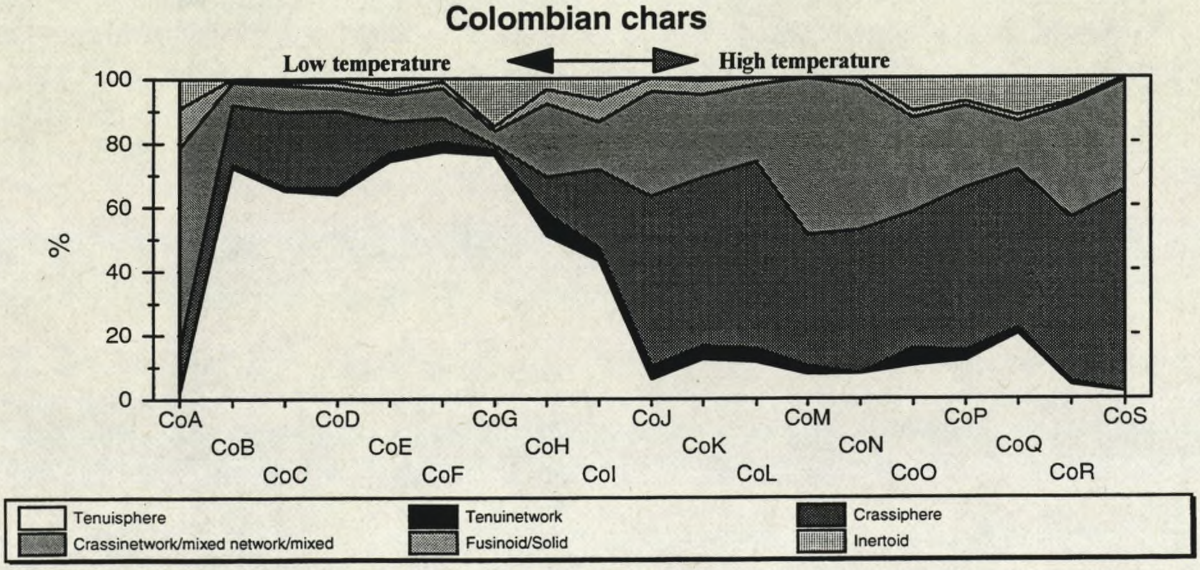

Figure 6.1 Chars derived from the Colombian coal type.

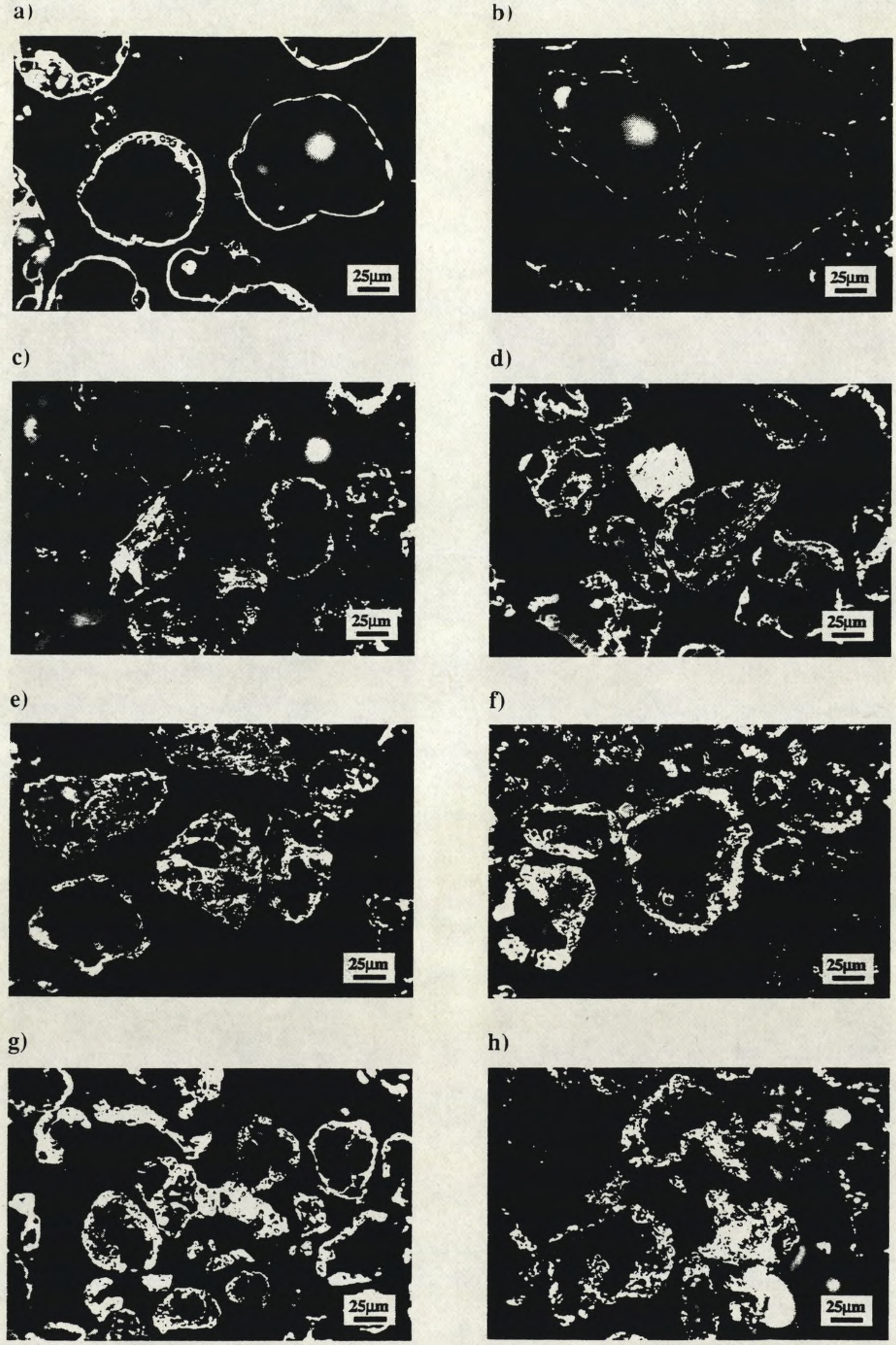

Figure 6.2 Photomicrographs of typical Colombian combustion chars, taken at a burnout at ~50-60 %.

The composition of the muffle furnace derived char sample (CoA) is significantly different from all other char samples, and is dominated by the mixed morphotype group. The appearances of the muffle furnace chars are very similar to coke used for steel production.

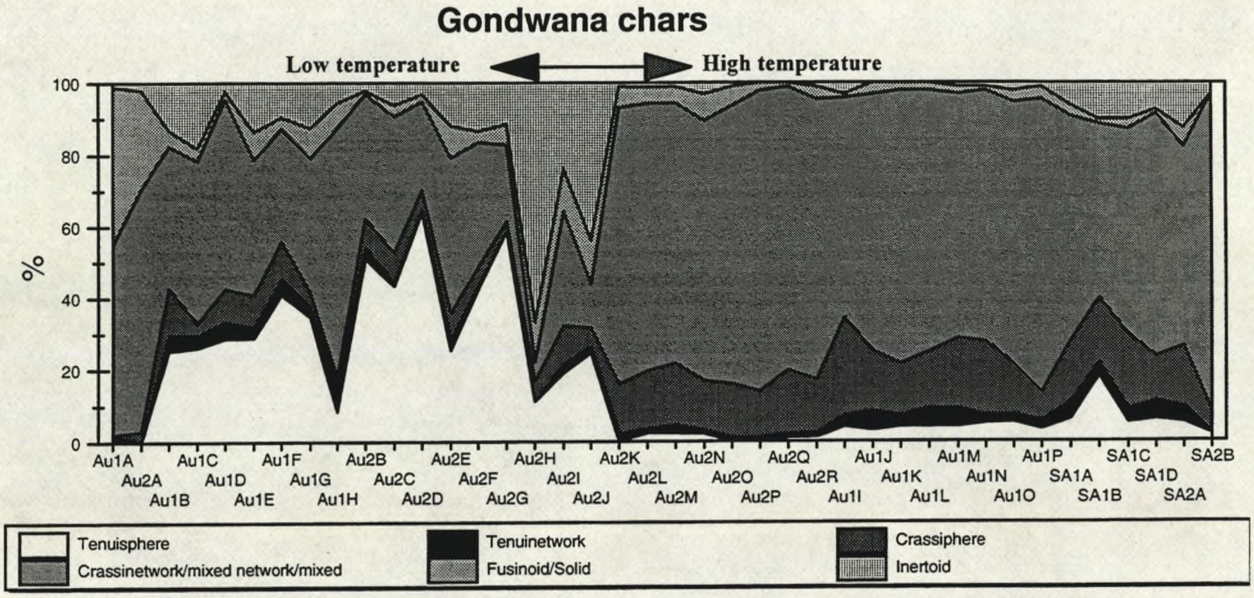

Figure 6.3 Chars derived from the Gondwana coal types.

The composition of the two DTF char samples produced at 1150 °C (CoH and CoI) is markedly closer to the composition of the high temperature char samples, with respect to the tenuisphere morphotype and the mixed morphotype group, than the low temperature DTF char samples. This relation is also illustrated by photomicrographs of chars with comparable burnout levels which are produced in the various reactors (Figure 6.2). It is evident that the two low temperature DTF chars are significantly different from the others, Figures 6.2 a & b. They are dominated by almost perfectly shaped, highly fused, thin-walled spheres, while the DTF chars produced at 1150 °C (Figure 6.2 c) are more complex in appearance, although still significantly different from the high temperature chars (Figures 6.2 d, e, f, g, h). The high temperature chars appear to be very similar in morphotype composition. They are all dominated by thicker-walled char morphotypes with small bubbles and generally they contain more vesicles. The presence of small bubbles in the wall has been suggested by Unsworth et al . (1991), to indicate pyrolysis after swelling has ceased. This phenomenon is apparently, strongly temperature dependant and we suggest that the more intense development of devolatilisation products at higher temperatures, together with a shorter period of plasticity, leads to the formation of bubbles.

All chars derived from the Gondwana coals are compared, since no single Gondwana coal has been tested in all reactors. The results are shown in figure 6.3. Although the coals are different in both rank and origin, some general trends can be extracted from the graphs. Again the composition of the low temperature DTF char samples (Au1B to Au1H and Au2B to Au2J) are markedly different from the high temperature samples, especially with respect to the tenuisphere and crassisphere morphotypes. Both the high and the low temperature char samples are rich in the mixed morphotype group, although the high temperature char samples are significantly richer in this group. As with the Çolombian char samples, only very few tenuinetworks are found and no clear trend in the distribution can be found. It is notable that the composition of the low temperature DTF char samples produced at 1150 °C (Au1H, Au2I and Au2J) approaches the composition of the higher temperature char samples.

The high temperature South African chars fit well into the group of high temperature Australian coal derived chars.

The chars produced in a muffle furnace (Au1A and Au2A) are significantly different from all other chars. They are richer in the denser char types (mixed morphotype group and the fusinoid/solid morphotypes), and are more like coke than combustion chars.

It is interesting to note the similarities in composition between high temperature char samples formed in laboratory scale and full scale experiments, indicating that in a laboratory scale reactor it is possible to produce chars very similar to those found in the flame zone of a p.f. combustion boiler.

As demonstrated above there is evidence that the char morphologies vary in a systematic way, dependant on the temperature domain in which they are produced. If the various char morphotypes are different with respect to reactivity and burnout characteristics, which we believe is the case, greater attention should be given to the experimental conditions under which the chars are produced. Thus the temperature and the heating rate should be very similar to the conditions in which the coals investigated are utilised. Preliminary results suggest a threshold temperature ~ 1300 °C for the production of chars comparable to full scale p.f. combustion chars. We believe that the higher intensity of the devolatilisation, perhaps combined with a shorter swelling time are the controlling factors in the development of denser char particles observed at higher temperatures.

6.2 Morphology and macroporosity development during burnout

6.2.1 Introduction

Vleeskens et al. (1993) have demonstrated that the morphotype development during combustion comprised very little variations until the latest stage in the combustion process. This may indicate that the various morphotypes burn at the same rate in the major part of the char combustion process, and contradict the general thesis that the various morphotypes burn at different rates as suggested by Bailey et al. (1990).

It was therefore decided to study the development of both the morphotypes and the macroporosity in the "Sandia" produced chars although these chars represent a relatively narrow burnout interval. These high-temperature laboratory chars are shown previously to closely reflect real p.f. combustion conditions.

The macroporosity is measured on individual particles in polished blocks using an image analysis system on the same polished cross sections as used for morphology determinations. The embedding material, and thus the internal pores, is eroded using the differences in grey level between this material and the char solid matter. After defining the particle outer surface and thereby eliminating exterior embedding material, the porosity is calculated as the area ratio between particle walls and vesicles. The resolution in separating pores from the solid material is estimated to be around 5 μm pore diameter. The process is extremely time consuming, and only 100 particles in each sample are measured, however this has proved to give representative results.

6.2.2 Development in char morphology during burnout

The development of the char morphologies as a function of the burnout is shown in Figures 6.4, 6.5 and 6.6. The values for the 6 and 12 % oxygen environments are separated as chars produced at various oxygen levels are not directly comparable, which is believed to be associated with the oxygen concentration influence on the char surface temperature.

Morphology determination has not been made on all the Colombian chars, Figure 6.4. In the 6% oxygen level there seems to be an enrichment of the tenuispheres with increasing burnout, and at the same time a decrease in the mixed group, while the dominant group, crassipheres, is unaffected. In the 12% environment no general trend can be observed, but as only two samples are represented, no firm conclusions can be drawn.

For the Australian coal 1 , Figure 6.5, in both 6 and 12 % environments, the two groups, crassipheres and crassinetwork/mixed network/mixed, dominate. The development with increasing burnout is parallel for the two oxygen levels, i.e. a weak decrease in the crassipheres group together with a small increase in the mixed group. The other groups are more or less unaffected.

The findings are in good agreement with Bailey et al. (1990), where the crassipheres were found to be more reactive than the crassinetwork/mixed network/mixed group. However the opposite development is observed with the Colombian coal in the 6% oxygen environment.

In Figure 6.6, the Australian coal 2 is shown. In both the 6% and the 12% oxygen environment, only a slight development can be observed with increasing burnout. The variations are in the same order of magnitude as the uncertainty of the measurements, and thus cannot be taken indicative although the burnout varies from 40 to above 70%.

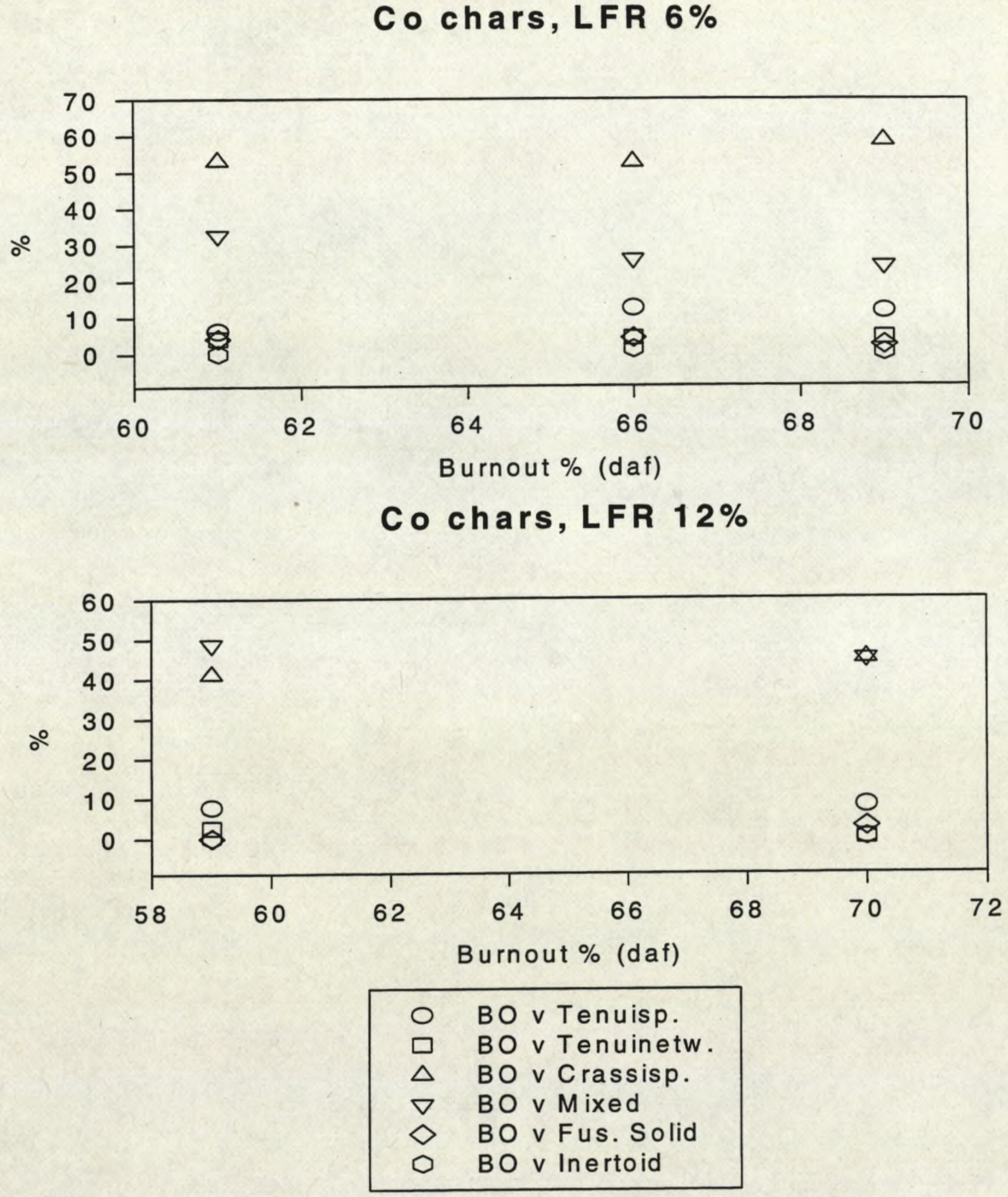

Figure 6.4 The morphotypes of the Colombian chars as a function of the burnout. The chars are sampled in the LFR in 6% and in 12% oxygen environments.

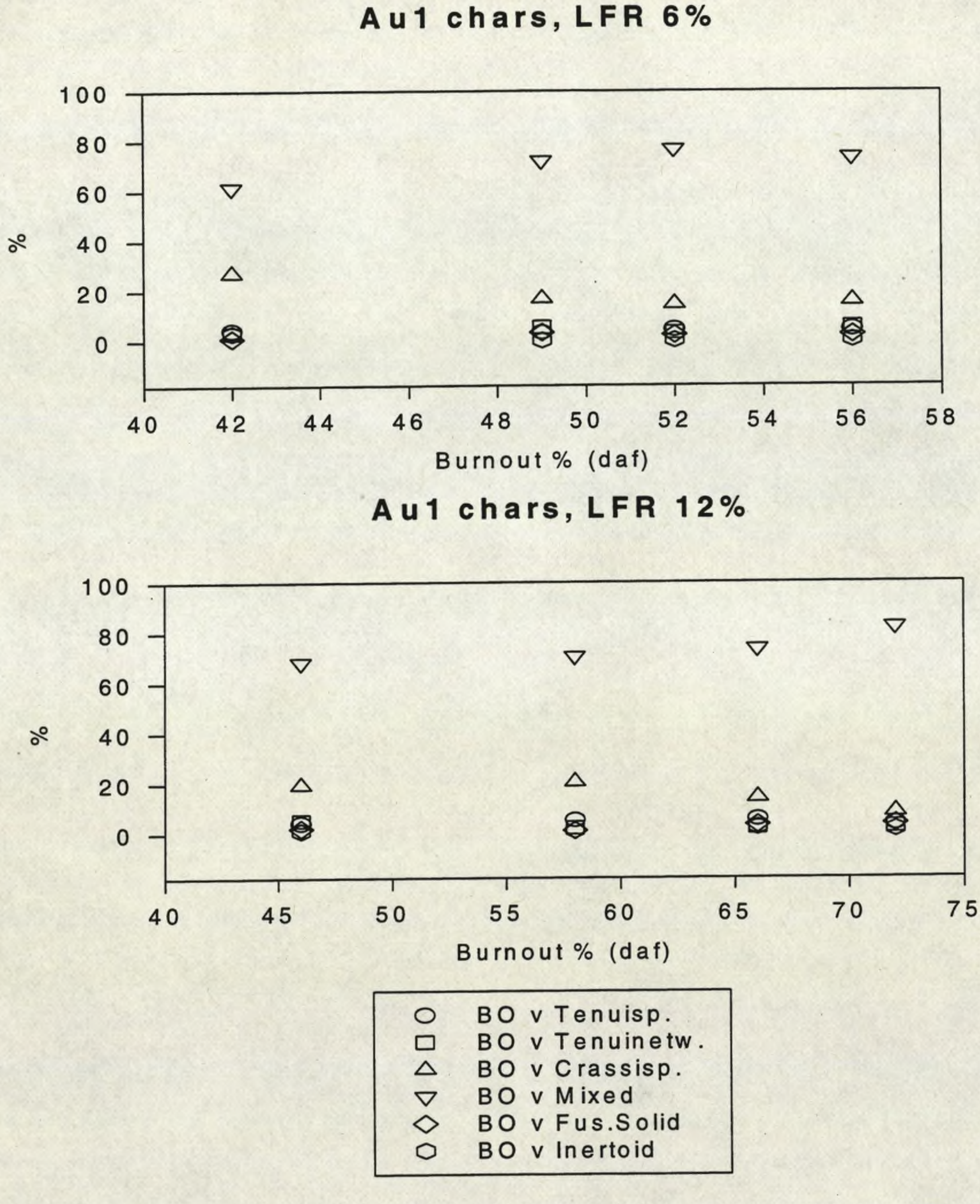

Figure 6.5 The morphotypes of the Au1 chars as a function of the burnout. The chars are sampled in the LFT in 6% and in 12% oxygen environments.

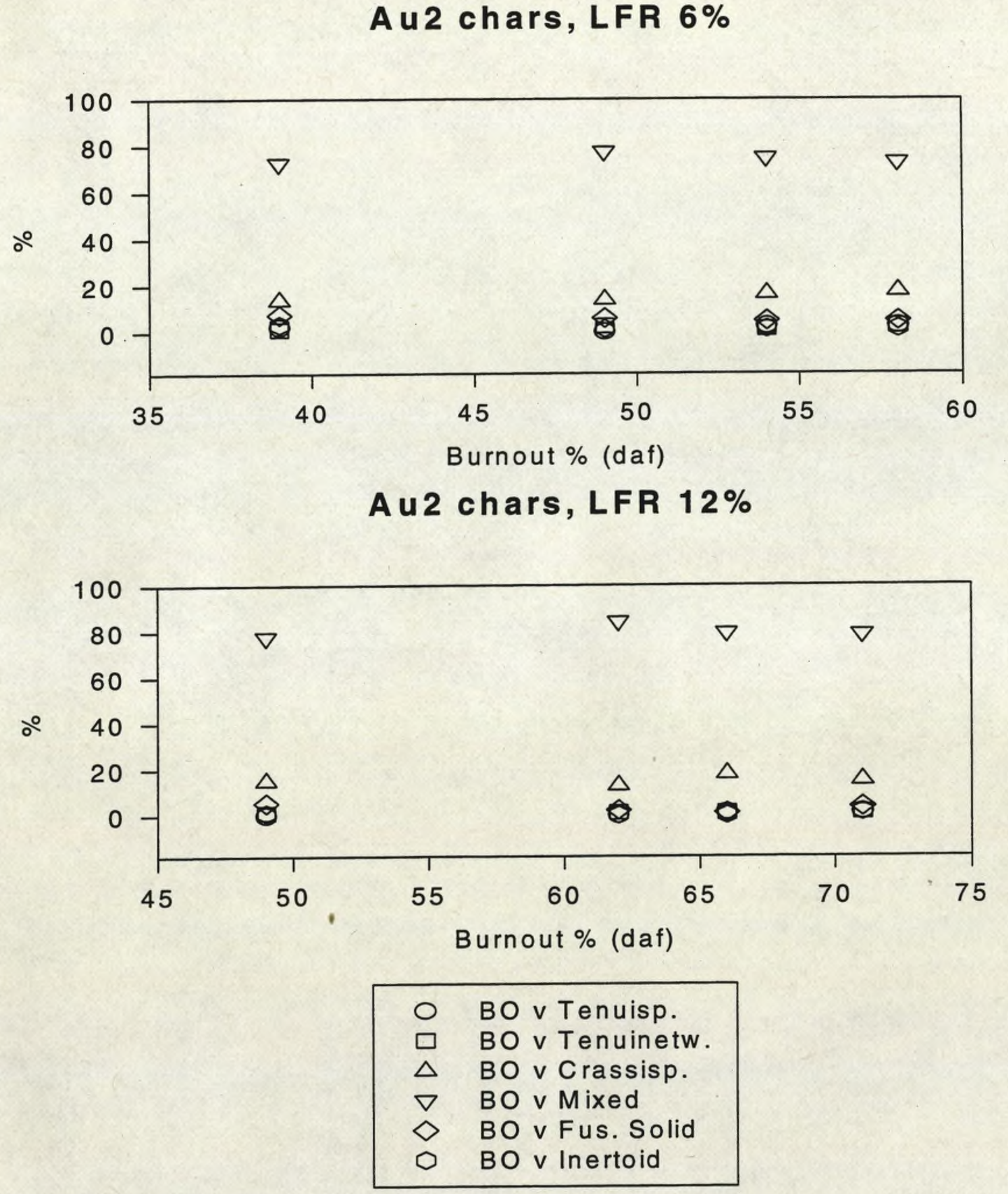

Figure 6.6 The morphotypes of the Au2 chars as a function of the burnout. the chars are sampled in the LFR in 6% and in 12% oxygen environments.

In general the data are not conclusive since we do not observe any morphotypes disappearing more rapidly than others. Only one of the Australian coal types seems to behave in compliance's with the general thesis on the reactivity of the various morphotypes (Bailey et al., 1990). One major problem is, off course, the complexity within the relatively simple groupings of the morphotypes. This is especially the case with the crassinetwork/mixed network/mixed group where the chars within this group represent a great variety in both morphology and porosity.

As mentioned above, these results on char morphology could lead to the conclusion that all the various morphotypes are burned out at the same rate, and that the morphologies of the chars play no role in the reactivity of the chars, in the present burnout interval, in agreement with the findings of Vleeskens et al. (1993). A uniform burning rate for the different morphotypes should however result in an increasing overall porosity, with the exception of the solid particles.

6.2.3 Char porosity as a function of the burnout

The overall porosity of the chars are shown in Figures 6.7 (Co), 6.8 (Au1) and 6.9 (Au2) as functions of the burnout (daf).

In the 6% oxygen environment, the Colombian Co chars do not change porosity at all, while in the 12 % oxygen environment, a significant change towards higher porosity is observed at the burnout levels 79% and 84%.

The porosity of the Australian Au1 chars is less uniformly distributed than the Colombian coal derived chars. Although the burnout span the interval from 42% to 72%, no clear trend can be observed, neither in the 6% or the 12% oxygen environment.

For the Australian Au2 chars the same comments are valid, with the exception that in the 12 % oxygen environment the char taken at a burnout of 71%, is markedly higher in porosity than the remaining Au2 chars.

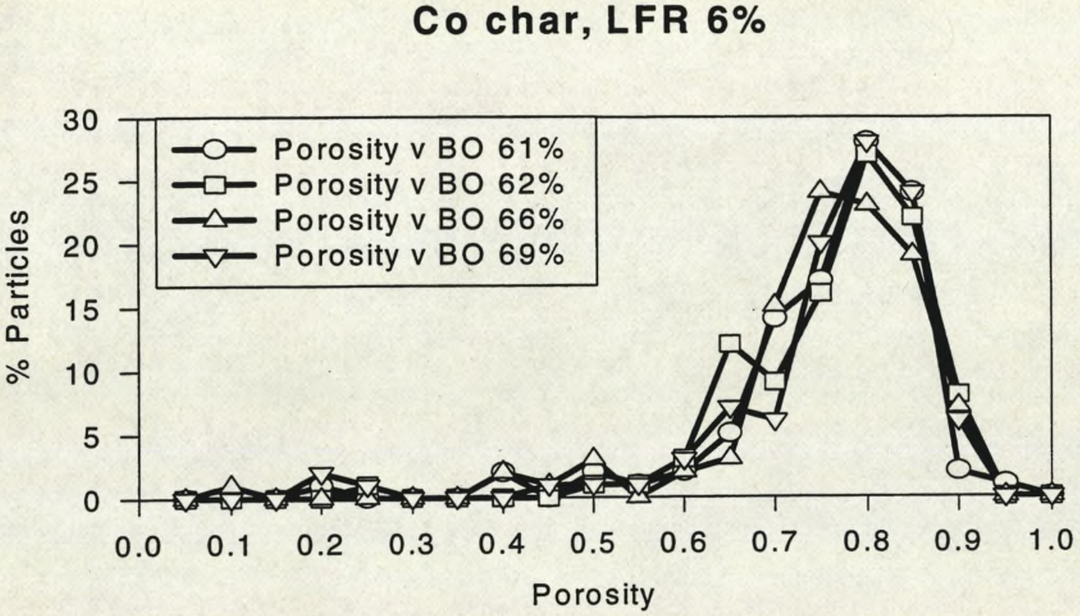

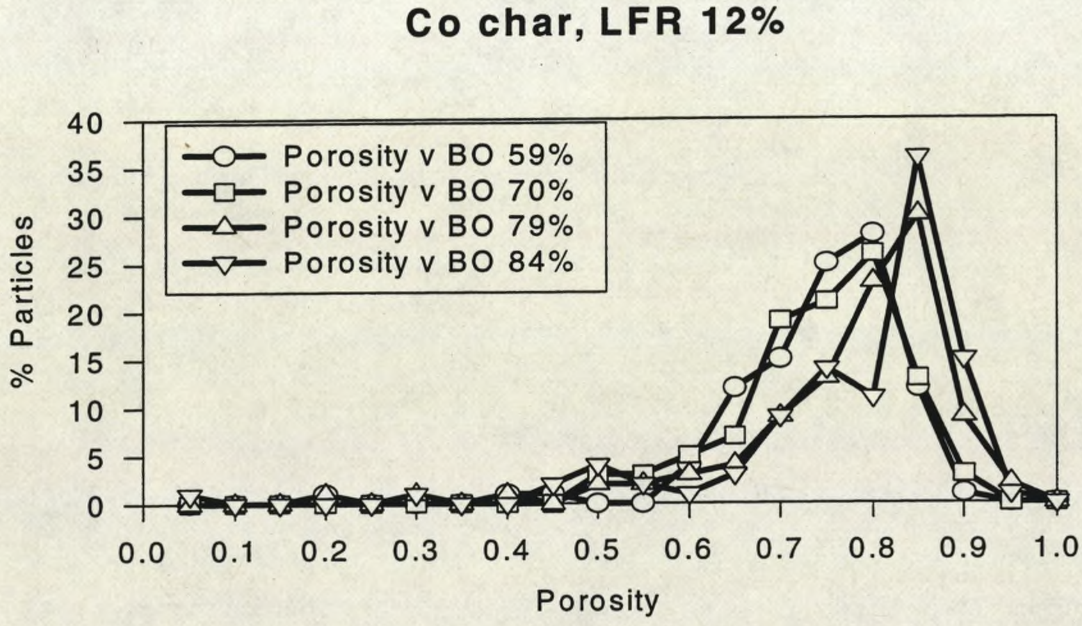

Figure 6.7 The overall porosity of the Co chars at various burnout(BO).

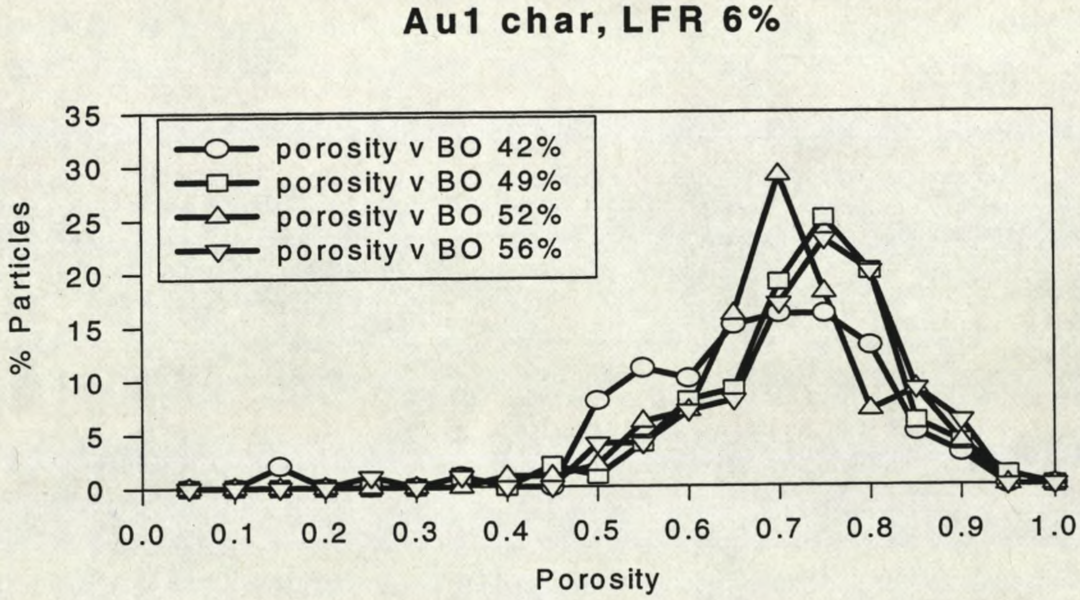

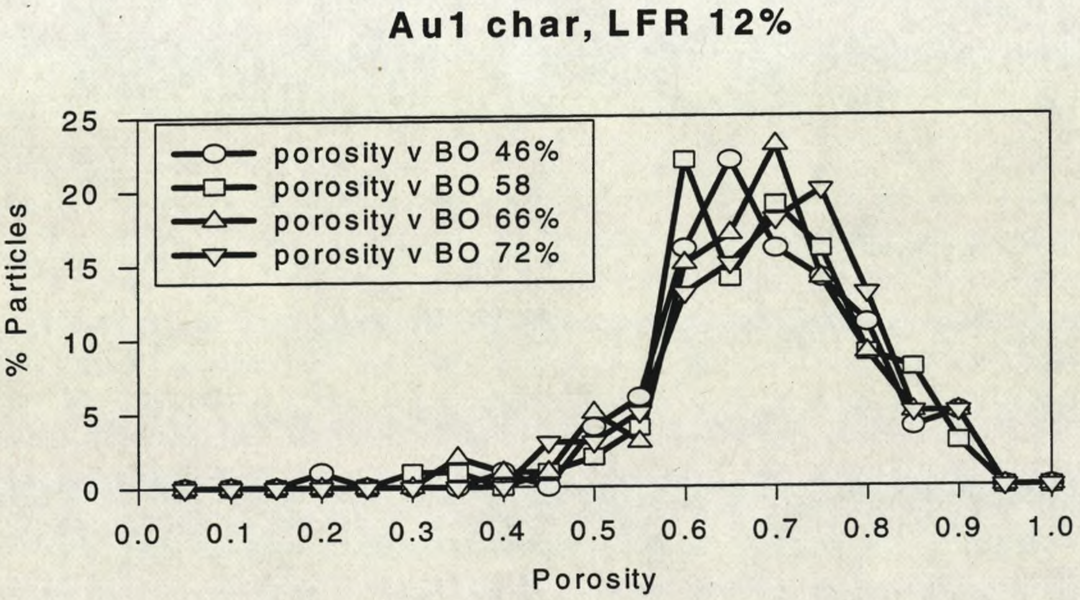

Figure 6.8 The overall porosity of the Au1 chars at various burnout(BO).

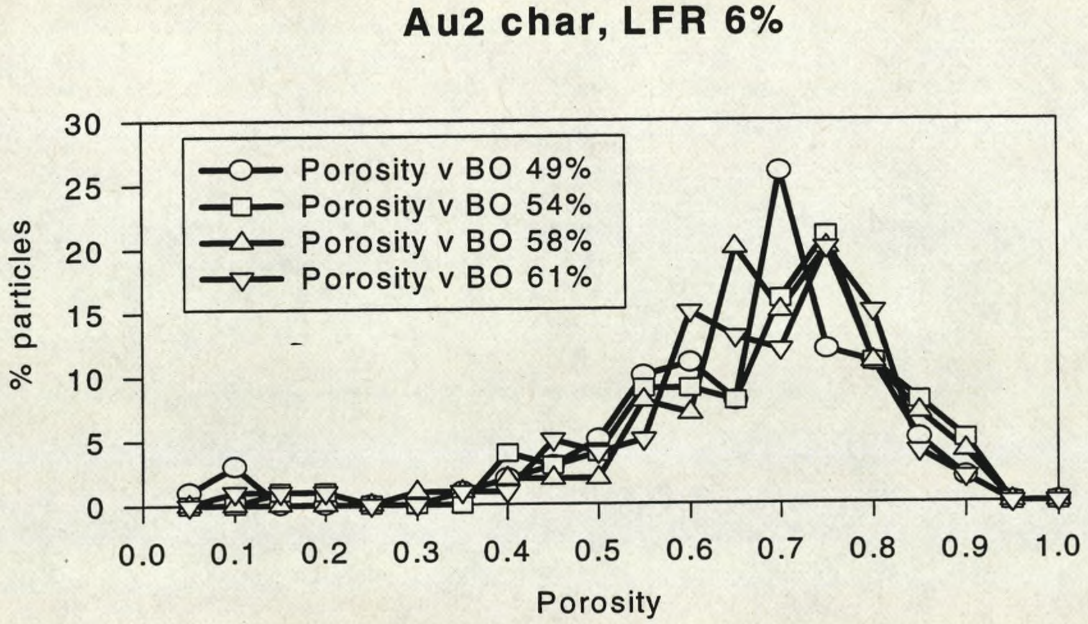

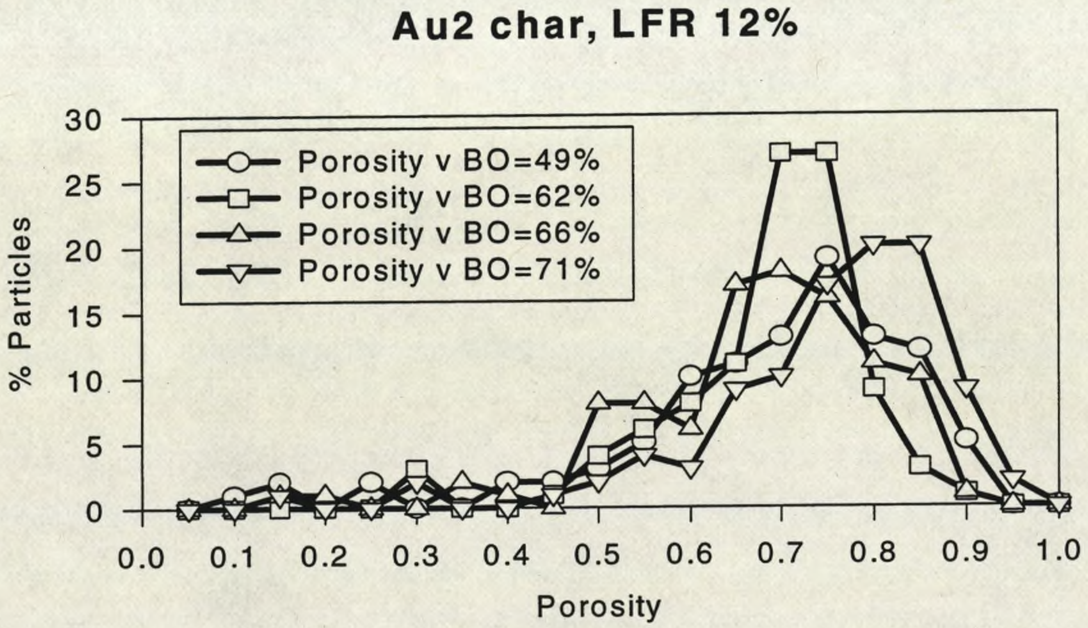

Figure 6.9 The overall porosity of the Au2 chars at various burnout(BO).

These results, together with the results on the morphotype development, leave us with no answer to what is happening in the middle interval of the burnout period. If the various particles burn out with the same mass loss rate, we should be able to observe a significant change in either the morphotypes or the overall porosity, which we cannot. As shall be demonstrated later in this report, it is obvious, that the present methods are too simple and lack sensitivity to fully describe the mass flow in the middle part of the reaction interval. It seems, however, that both the texture and the porosity change significantly during the final stage of char combustion (>70% burnout)(Fig 6.9).

6.3 Discussion and conclusion

Systematic variations in the texture of chars produced in different temperature domains from the same Colombian coal were found. Similar variations have been found in chars produced from a suite of Gondwana coals, even though these coals differ in both rank and origin. These results suggest that the temperature is a dominant factor in the formation of the different char morphotypes. Thus experimental work in the scope of correlations between the coal petrography and char morphology, and determination of char reactivity and burnout characteristics, should only be accomplished on chars produced at realistic temperatures, i.e. similar to those for the intended use of the coal. The results suggest a threshold temperature of ~1300 °C for producing char morphologies comparable with those produced in a p.f. combustion boiler.

In the burning interval from ~40% to 70% burnout, the classical petrographic methods to determine the morphology and the porosity cannot adequately describe the mass flow. As will be demonstrated in this report, more sensitive and sophisticated methods need to be developed. However, in the final stage of the combustion significant changes in both the morphology and in the porosity are observed by classical methods.

7 CHAR MORPHOLOGY RELATED TO COAL PETROGRAPHY

7.1 Introduction

Burnout behaviour of coal during pulverised fuel (p.f.) combustion in power plants is known to be influenced by the reactivity of chars produced at the early stage of the combustion process (Jones et al., 1985). Therefore the relationship between char morphology and the petrographic composition of parent coal has been studied by several workers in this field in order to predict the burnout behaviour of a feed coal with a particular petrographic composition (Jones et al., 1985; Falcon and Ham, 1988; Goodarzi and Vleeskens, 1988; Bailey et al., 1990; Bend et al., 1991; Gentzis and Chambers, 1993).
Rosenberg et al. ,1996 (see also chapter 6) demonstrated that the char morphotypes derived from combustion are highly influenced by temperature conditions, and only combustion of coal at temperatures higher than approximately 1300 °C forms an assemblage of char morphotypes comparable to full scale p.f. combustion. Correlations between low temperature (< ≈1300 °C) chars and the parent coal petrography is therefore not justified as these char morphotypes do not reflect realistic combustion conditions (Rosenberg et al. 1996). Therefore, only high-temperature chars derived from full scale p.f. combustion in power plants and from combustion close to the conditions in full scale experiments were used to perform correlation between char morphology and parent coal petrography in the present study (Table 7.1). Some studies have dealt with the morphology of chars derived from pyrolysis of maceral concentrates (Jones et al., 1985; Crelling et al., 1988; Thomas et al., 1993). We believe, however, that a realistic approach is to focus on the pulverised raw coal as this reflects the fuel actually used in p.f. combustion.

Char reactivity is supposed to be related to the porosity of the chars, and a correlation between high-porosity chars and a specific coal petrographic composition may thus be of particular interest. This chapter demonstrates some general relationships between the morphology of the high-temperature chars and the parent coal petrography.

Char sample	Reactor type	% Burnout	Sample position	Temperature °C
CoJ	Laminar flow reactor	61	64 mm (47 ms)	1409 (6% O2)
CoM	Laminar flow reactor	59	64 mm (47 ms)	1419 (12% O2)
CoP	Full scale	63	Flame zone	c. 1500
CoR	1.5 MW tunnel reactor	50	-	c. 1300-1400
CoS	Entrained flow reactor	52	250 ms	1330
Au1J	Laminar flow reactor	49	129 mm (72 ms)	1369 (6% O2)
Au1K	Laminar flow reactor	52	191 mm (95 ms)	1320 (6% O2)
Au1L	Laminar flow reactor	56	254 mm (117 ms)	1263 (6% O2)
Au1N	Laminar flow reactor	58	129 mm (72 ms)	1372 (12% O2)
Au2K	Laminar flow reactor	49	64 mm (47 mm)	1409 (6% O2)
Au2L	Laminar flow reactor	54	129 mm (72 ms)	1369 (6% O2)
Au2M	Laminar flow reactor	58	191 mm (95 ms)	1320 (6% O2)
Au2N	Laminar flow reactor	61	254 mm (117 ms)	1263 (6% O2)
Au2O	Laminar flow reactor	49	64 mm (47 ms)	1419 (12% O2)
SA1A	Full scale	49	Flame zone	c. 1500
SA1C	Full scale	61	Flame zone	c. 1500
SA2B	Entrained flow reactor	52	250 ms	1330
PoA	Full scale	63	Flame zone	c. 1500
PoC	Full scale	61	Flame zone	c. 1500

Table 7.1 High temperature char samples with burnout c. 50%-60%.

7.2 Coal sample preparation and methods

Each coal sample was crushed to a grain size of approximately 5 mm and subsequently homogenised, and split into four parts of which two were removed. The remaining two parts were homogenised and the splitting procedure was repeated until about 100 grams of coal was achieved. This coal was crushed to the fraction 63-1000 μm (analysis fraction). If the fraction <63 μm amounted to more than 10% of the 63-1000 μm fraction, about 20% of the coal <63 μm was blended with the analysis fraction.

Approximately 18 ml of the analysis fraction was embedded in epoxy and after hardening cut vertically into two pieces. The "new" face was ground and polished using 1/4 μm diamond powder for the final polish to obtain a smooth surface.

The rank of the coals was determined by means of random reflectance measurements on collotelinite. This is in accordance with the standards outlined in Stach et al. (1982). The equipment used was a Leitz MPV-SP system, which was calibrated against a standard with a reflectance of 0.893 %Ro. A total of 100 measurements per sample was conducted in monochromatic light and oil immersion.

Automatic image analysis (PIA system, Technisches Büro Hilgers) was used to measure the **t**otal **r**eflectance **d**istributions (TRD) of the coal samples. The PIA system consists of a reflected light microscope equipped with a high sensitive TV-camera, and an automatic scanning stage and autofocusing device. The system is calibrated as described above. A measurement with the image analysis system detects the grey level distribution in the coal and thus enables a mapping of semi-inert transitions between vitrinite and inertinite.

Combined maceral-microlithotype analysis, which detects associations of macerals (microlithotypes) and maceral group distributions, was used to determine the petrographic composition of the coals. The analyses were carried out in oil immersion using a Zeiss incident light microscope equipped with visible and ultraviolet light sources and a Swift point counter. A 20 point graticule was inserted in the eye piece and an intersection was chosen as fixpoint in order to determine which maceral group should be counted. Two conversions were fulfilled during the microlithotype analysis which gives a quantitative estimation of the maceral associations in the coal (Stach et al., 1982): 1) the band width of the microlithotype must be at least 50 μm; and 2) a maceral group represented by less than 5% by volume was disregarded. The distance between the outermost intersections on the 20 point graticule is 50 μm allowing an easy observation of the band width, and each of the 20 intersections of the graticule corresponds to 5% by volume allowing easy recognition of the 5% by volume limit. To be recorded as a microlithotype at least 10 intersections had to fall within a particle while the fixpoint determined which maceral group/maceral type had to be counted. If the fixpoint fell outside the particle the microlithotype was recorded as an "observed microlithotype", but if the fixpoint fell within a maceral without 10 intersections situated inside the particle the maceral was recorded as a "maceral at the boundary". 500 points (microlithotypes and maceral types) were recorded in each sample. The definitions of the different microlithotypes are shown in Table 7.2.

Microlithotype	**Maceral group composition**
Vitrite	vitrinite >95%
Liptite	liptinite >95%
Inertite	inertinite >95%
Clarite	vitrinite+liptinite >95%
Vitrinertite	vitrinite+inertinite >95%
Durite	inertinite+liptinite >95%
Trimacerite	vitrinite, inertinite, liptinite >5%
-Duroclarite	vitrinite > inertinite, liptinite
-Clarodurite	inertinite > vitrinite, liptinite
-Vitrinertoliptite	liptinite > vitrinite, inertinite

Table 7.2 Definition of microlithotypes.

7.3 Origin and petrographic composition of the parent coals

Six coal samples were used, including one coal blend: a Colombian coal sample (Co), two Australian coal samples (Au1 and Au2), two South African coal samples (SA1 and SA2) and a Polish coal blend sample (Po).

The Colombian sample is a Tertiary coal from a coalfield in the north-eastern part of Colombia. It is from a 900 m thick, coal-bearing formation, which contains up to 55 coal seams with thichnesses ranging up to 26 m (Walker, 1993). It has a mean random reflectance of 0.59 %Ro indicating a high volatile bituminous C rank (Table 7.3). It has a high vitrinite content and is dominated by vitrinite-rich microlithotypes (Table 7.3). This is also reflected on the TRD curve showing a well-defined peak in the vitrinite reflectance range (Figure 7.1). The transition to the inertinite macerals is distinct without any pronounced proportion of components with intermediate reflectances.

Coal sample composition(vol. %)

Petrography	Co	Au1	Au2	SA1	SA2	Po
Vitrite	21	6	7	7	7	30
Inertite	6	23	17	44	38	14
Clarite	25	0	2	2	2	8
Durite	0	8	2	16	21	4
Vitrinertite	19	30	33	17	11	12
Duroclarite	25	9	14	3	7	13
Clarodurite	1	23	23	7	9	4
Vitrinertoliptite	0	0	0	1	0	0
Carbominerite	3	1	2	3	5	15
Vitrinite	75	27	37	20	20	54
Liptinite	6	3	7	3	6	5
Inertinite	17	69	54	75	72	28
Minerals	2	1	2	2	2	13
%Ro	0.59	0.62	0.63	0.80	0.71	0.74/1.03

Table 7.3 Petrographic composition of the coals.

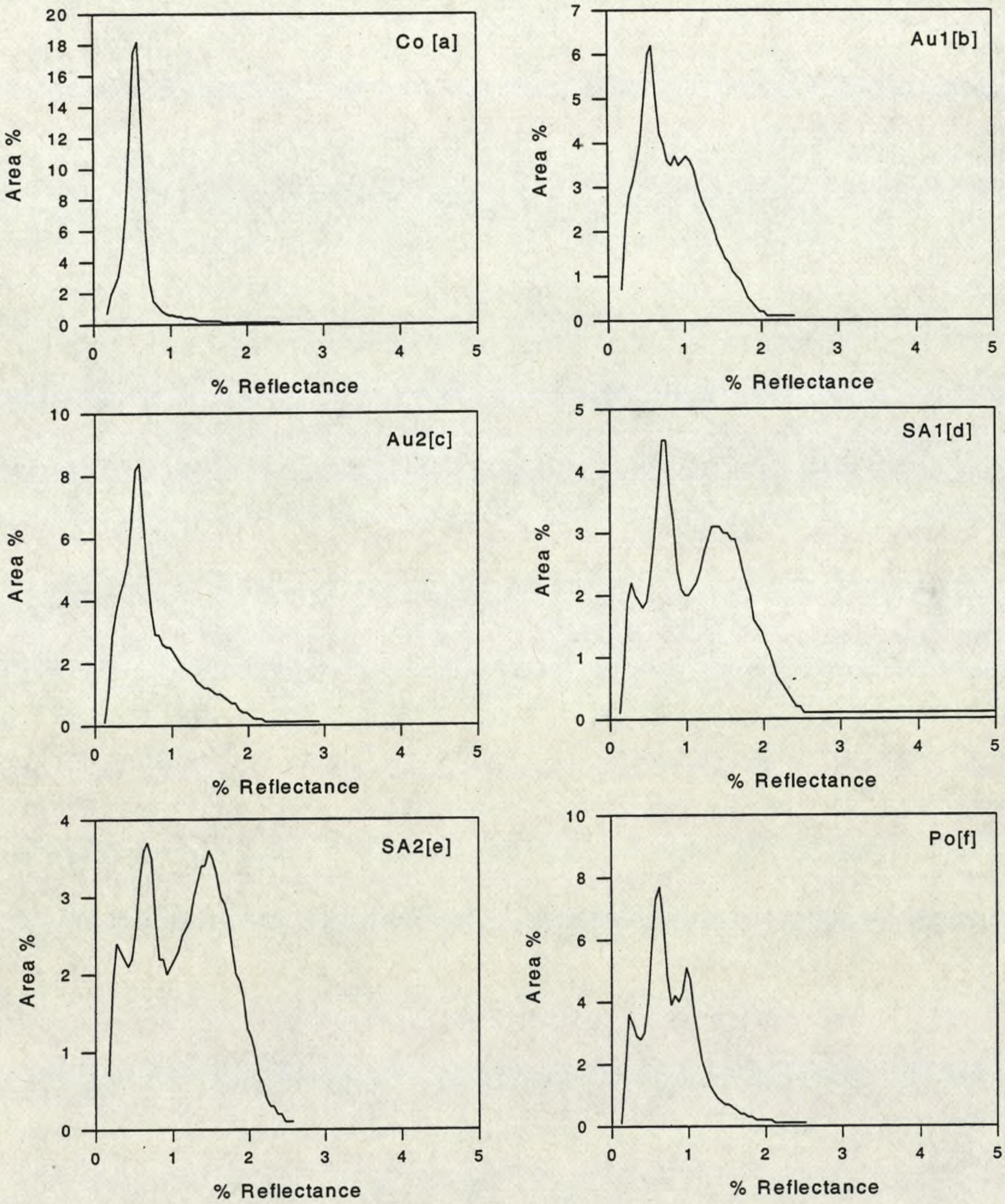

Figure 7.1 Total reflectance distribution for the six feed coals.

The four Permian Australian and South African coals were deposited in the ancient southern Gondwana continent that comprised South America, South Africa, Antarctica, Australia and India. The precursor peat's of these coals were formed in a cold to cool temperate climate which together with slow subsidence of the depositional areas favoured oxidation of the plant tissues (Hobday, 1987; Martini and Johnson, 1987; Hagelskamp and Snyman, 1988; Holland et al., 1989; Hunt, 1989; Hunt and Smyth, 1989; Taylor et al., 1989). This resulted in inertinite-rich coals. The two Australian coals, Au1 and Au2, are both of high volatile bituminous C rank (Table 7.3). They are characterised by a high proportion of inertinite exhibiting a wide range of reflectance's transitional between vitrinite and inertinite. These semi-inert macerals are shown on the TRD curve as a prominent "shoulder" on the right limb of the main peak which corresponds to the vitrinite reflectance range (Figure 7.1). This semi-inertinite may be regarded more reactive than the high reflecting inertinite due to a higher hydrogen content (higher H/C ratio) (Diessel, 1983). The high content of semi-inertinite/inertinite macerals is reflected in the dominance of inertinite-rich microlithotypes like inertite, vitrinertite and clarodurite (Table 7.3).

Reflectance measurements indicate a high volatile bituminous B rank for the South African SA2 coal and high volatile bituminous A rank for the South African SA1 coal (Table 7.3). Both samples are dominated by an extremely high proportion of the inertinite maceral group and of inertinite-rich microlithotypes (Table 7.3). The TRD curves are characterised by three peaks (Figure 7.1). The peak to the right in the high reflectance range represents the inertinite fraction and illustrates, that a major part of the inertinite macerals are semi-inert and have reflectance's transitional between vitrinite and inertinite. This suggests that a significant part of the inertinite fraction may be partly fusible. The middle peak represents the vitrinite macerals, whereas the very left peak is situated within the reflectance range of liptinites, mineral matter and low reflecting, commonly fluorescing, vitrinite collodetrinite (detrital vitrinite).

The Polish coal is the only blend in this study. It is probably a blend of a high volatile bituminous B coal (mean random reflectance, 0.74 %Ro) and a high volatile bituminous A coal (mean random reflectance , 1.03 %Ro) (Table 7.3). The coal blend is dominated by vitrinite but contains also a significant proportion of inertinite, which is shown by the microlithotype composition. The TRD curve shows three peaks. The population to the right is probably related to the higher reflecting vitrinite in the high volatile bituminous A coal and the inertinite in both coals in the blend. This is in contrast to the South African coals where the right peak is attributed to semi-inert components.

7.4 Correlation between char morphology and feed coal petrography

Of the 63 char samples in this study a total of 36 are high temperature chars, which were used for correlation to the feed coal petrography. At a burnout (d.a.f.) of approximately 50-60% the chars are taken to be completely pyrolysed/devolatilised. Nineteen high temperature char samples representing this burnout level have been produced (Table 7.1). However, the different reactor or full scale experiments have produced several char samples from the same feed coal with a burnout level of ≈50-60%. A normalised composition of the SA2 derived char (AvSA2) together with five normalised average char compositions (AvCo, AvPo, AvAu1, AvAu2, AvSA1) were calculated from these samples (Table 7.4). The average compositions are used for correlation to the coal petrography of the parent coals.

Average char composition

Char type	AvCo	AvAu1	AvAu2	AvSA1	AvSA2	AvPo
Tenuisphere	9	4	1	9	2	24
Tenuinetwork	3	4	2	4	0	6
Crassisphere	54	17	15	17	6	31
Crassinetwork/Mixed network/Mixed	30	73	74	64	89	29
Inertoid	4	2	6	5	3	6
Fusinoid/Solid	0	2	2	1	0	4
Number of samples	5	4	5	2	1	2

Table 7.4 Average composition of the char samples.

Classification of the char morphotypes reveals some clear differences between the samples, in particular between the chars derived from the Colombian coal (AvCo) and the Polish coal blend (AvPo), and the chars derived from the Australian and South African coals (AvAu1, AvAu2, AvSA1, AvSA2) (Table 7.4). The AvCo sample is dominated by the crassisphere morphotype, which are high-porosity chars with few prominent degassing pores (Figure 7.2a, b). Second is the group comprising crassinetwork and mixed morphotypes. Likewise, the highly porous tenuisphere morphotype is present in a significant proportion (Table 7.4; Figure 7.2c).

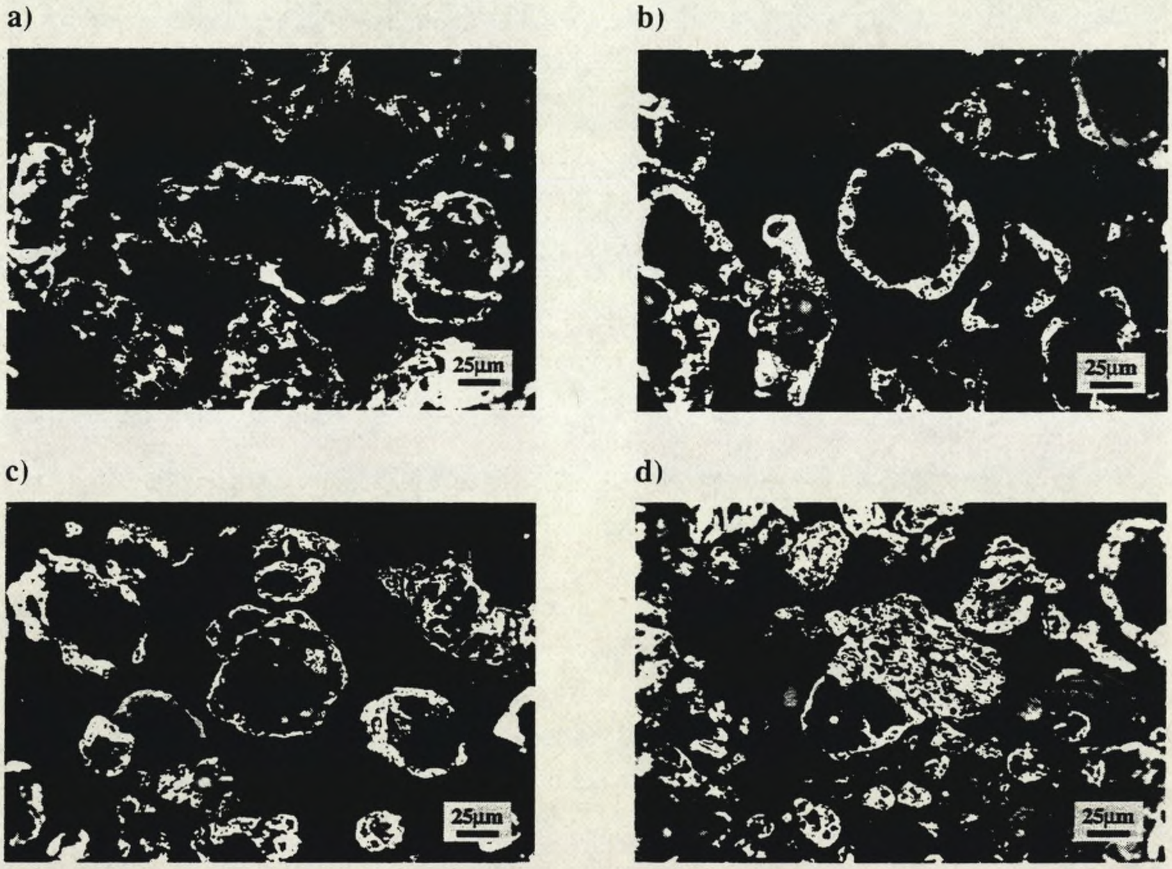

Figure 7.2 Examples of char morphotypes: (a) and (b) crassiphere chars (AvCo); (c) tenuisphere char (AvCo); (d) mixed network char (AvSA2).

The AvAu1 and AvAu2 samples derived from the Australian coals are dominated by a high proportion of the crassinetwork/mixed char group, followed by the crassisphere morphotype (Table 7.4; Figure 7.2a, b). The other char types are subordinate. The South African AvSa1 and AvSA2 samples are dominated likewise by the crassinetwork and mixed char types (Figure 7.2d), in particular the AvSA2 sample where the content is very high (Table 7.4). The AvSA1 sample is comparable to the Australian samples by having a pronounced proportion of the crassisphere morphotype. In contrast, the AvSA2 sample contains only subordinate proportions of the highly porous tenuisphere, tenuinetwork and crassisphere char types.

The Polish coal blend char, AvPo, is somewhat intermediate in composition, having a high proportion of the crassisphere and tenuisphere morphotypes and the crassinetwork/mixed group of chars.

A principal component analysis has been carried out using the computer programme Sirius (Kvalheim and Karstang, 1987). The 36 high temperature char samples, containing 6 morphotypes, were loaded into the data matrix allowing a two principal component model to be extracted. The model explains almost 98% of the total variance in the date set, thus losing only c. 2% of the information. The score plot of the date set shows a two-dimensional representation of the variance, explained by the multivariate model of the date set (Figure 7.3). Thus the overall similarities among the char samples can be studied and clustered. The separation in the Principal Component 1 (PC1) direction is prominent and separates the Australian/South African samples from the Colombian/Polish samples. In the Principal Component 2 (PC2) direction, a weaker separation of the South African and Australian samples can be observed together with a weak separation between the Colombian and Polish samples. The Australian char samples were only produced in one reactor type and are thus very similar, in contrast to the Colombian char samples which were produced from different reactors and, consequently, have higher variances. Nevertheless, a good separation between the four groups can be observed indicating a good correspondence between the petrography of the feed coal and the resulting char morphology. The separation in the PC1 direction may be explained by the different petrographic composition of the parent coals, whereas the separation in the PC2 direction may be caused by differences in rank, as already indicated by the petrographical analyses. However, the low number of feed coals does not allow a statistical valid conclusion to be made. One South African sample fall in the field of the Australian samples; this cannot be explained and may be incidental. Thus, in the case of the coals in this study, the most significant controlling factor on the char composition appears to be the petrographic composition of the parent coals. This is notable as the char morphotypes seem to determine the reactivity of the chars. In the following the relationship between the petrographic constituents of the coal and the char morphotypes will be described in more detail in order to detect the petrographic composition which results in the most reactive char morphotypes.

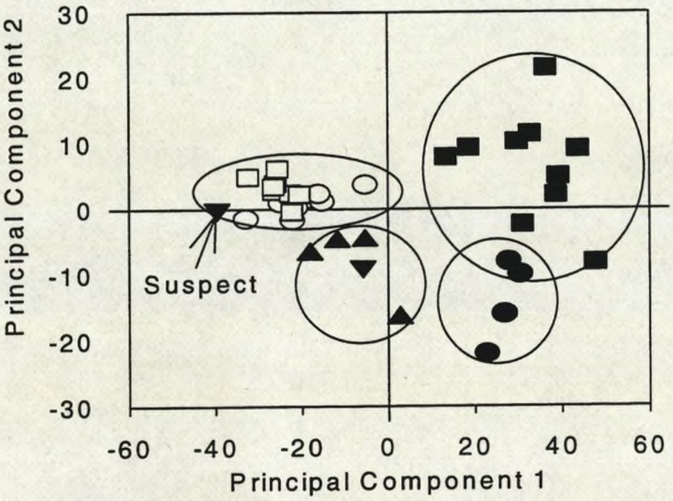

Figure 7.3 Score plot from the principal component analysis of the high-temperature chars, showing the major variances in the data set projected on the two principal components; ■ : Co chars; ○ : Au1 chars; □: Au2 chars; ▲ : SA1 chars; ▼ : SA2 chars; ● : Po chars.

The Colombian coal and the Polish coal blend are characterised by a high proportion of the vitrinite-rich microlithotypes vitrite, clarite, and vitrinertite V, and this seems to have favoured the formation of the crassisphere morphotype, but also tenuisphere chars. The proportion of the three microlithotypes in the Colombian coal amounts to 57 vol.%, and the average content of crassispheres in the AvCo char sample is 54% (Table 7.5, Figure 7.4); if the tenuisphere chars are included the value is 63% (Table 7.5). In the Polish coal blend the three microlithotypes amount to 44%, whereas the AvPo char sample contains 31% of crassispheres (Table 7.5, Figure 7.4). If the tenuisphere morphotype is included the value increases to 55%, thus emphasising the high proportion of tenuisphere chars produced by the coal blend. In the Australian and South African coals with low proportions of the vitrinite-rich microlithotypes, corresponding low proportions of the crassisphere morphotype are produced during combustion. The two Australian feed coals, Au1 and Au2, contain 15% and 20 vol.% of vitrite, clarite and vitrinertite V respectively, and the two resulting chars, AvAu1 and AvAu2, contain 17% and 15% of the crassisphere morphotype, respectively (Table 7.5, Figure 7.4). The South African SA1 coal contains 15 vol.% of these microlithotypes, whereas 17% of the crassisphere morphotype is present in the AvSA1 sample. The values for the SA2/AvSA2 samples are 13 vol.% and 6% respectively (Table 7.5, Figure 7.4). Due to the generally low proportion of tenuisphere chars derived from the Australian and South African coals, the results are not significantly altered by including this morphotype (Table 7.5). These results suggest a general relationship between the vitrite+clarite+vitrinertite V microlithotypes and mainly the crassisphere morphotype, but also the tenuisphere morphotype. The relationship is particularly pronounced for vitrinite-rich coals. This is in agreement with the results by Bailey et al . (1990); however, these authors found also a strong, rank dependent correlation to tenuinetwork chars. None of the present coals have produced significant proportions of the tenuinetwork morphotypes, and thus our study can not confirm this correlation.

The proportion of crassinetwork and mixed morphotypes is very high in the four inertinite-rich coals from Australia and South Africa. The total sum of inertite, durite, vitrinertite I, duroclarite and clarodurite in the Au1, Au2, SA1 and SA2 coals is 80 vol.%, 71 vol.%, 79 vol.% and 81 vol.% respectively. The proportion of the crassinetwork/mixed morphotype group in the corresponding char samples, AvAu1, AvAu2, AvSA1 and AvSA2, is 73%, 74%, 64% and 89%, respectively (Table 7.5, Figure 7.4). A correlation may be seen, but the SA1/AvSA1 is an outlier. It may be suggested that a higher proportion of crassisphere plus tenuisphere morphotypes was formed despite the inertinite-rich composition of the SA1 coal. The Colombian coal shows a good correspondence between the microlithotypes and char types: 38 vol.% and 30% (Table 7.5, Figure 7.4). The correlation between the Polish coal blend and the AvPo char sample is less satisfactory being 39 vol.% and 29% respectively (Table 7.5, Figure 7.4). Extraordinary high content of the dense inertoid and fusinoid/solid morphotypes was not observed in the Australian and South African chars despite the high inertinite content of the feed coals, which may be related to the semi-inert character of the inertinite. Bailey et al. (1990), correlated durite and inertite to inertoid, mixed, solid and fusinoid morphotypes. The char samples derived from the present parent coals rich in the microlithotype inertite, do not contain equivalent proportions of the inertoid, mixed, solid and fusinoid char types, and thus it has not been possible to demonstrate that correlation.

Microlithotypes/Char morphotypes	Co/AvCo	Po/AvPo	Au1/AvAu1	Au2/AvAu2	SA1/AvSA1	SA2/AvSA2
Vitrite+Clarite+Vitrinertite V	57 vol.%	44 vol.%	15 vol.%	20 vol.%	15 vol.%	13 vol.%
Crassisphere	54%	31%	17%	15%	17%	6%
Crassisphere+Tenuisphere	63%	55%	21%	16%	26%	8%
Inertite+Durite+Vitrinertite I+ Duroclarite+Clarodurite	38%	39 vol.%	80 vol.%	71 vol.%	79 vol.%	81 vol.%
Crassinetwork/Mixed network/Mixed	30%	29%	73%	74%	64%	89%

Table 7.5 Correlation between feed coal petrography and char morphology.

The results from this coal date set indicate that a correlation between vitrinite-rich microlithotypes and high-porosity chars exist. As the porosity of the chars is related to the reactivity , the formation of char morphotypes with high-porosity may have implications for the burnout, in particular in the final stages of burnout. It is therefore notable that the Polish coal blend produces the highest proportion of high-porosity chars (24% tenuispheres and 31% crassispheres), which could be related to the rank. The score plot suggests that the rank influences the char morphology, and it must therefore be noted that this factor may account for some of the discrepancies in the correlations between the petrographic composition of the feed coals and the resulting char morphology. It is probably necessary to consider the rank to strengthen the correlation.

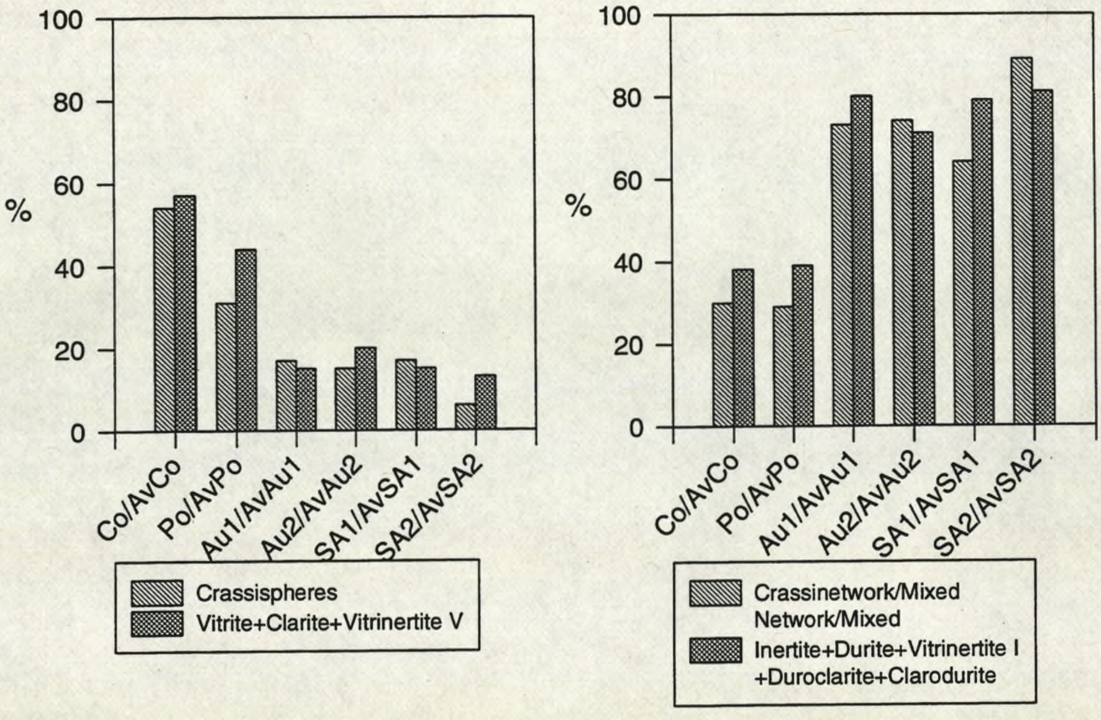

Figure 7.4 Histograms showing the correlation between coal microlithotypes and char morphotype groups.

7.5 Conclusions

A general correlation between the petrography of the coals, and the morphology of their high-temperature derived combustion chars has been demonstrated. A minor effect from the coals' rank may be observed, however, the present rank span is too narrow and the number of coals studied too small to allow any statistical valid conclusions to be drawn.

Particularly vitrite, clarite and vitrinertite V may in particular be correlated with the porous crassisphere morphotype, and probably also with the tenuisphere morphotype, inertite, durite, vitrinertite I, clarodurite and duroclarite microlithotypes may be correlated with the crassinetwork/mixed network/mixed morphotype group.

One of the difficulties in establishing a more detailed correlation lies in the crassinetwork/mixed network/mixed morphotype group, which contains a wide range of morphologies and porosities.

8 SCANNING ELECTRON MICROSCOPY

8.1 *Introduction*

Scanning Electron Microscopy (SEM) is a strong tool for providing morphological information about the particulate material as well as relative compositional variations. In many ways this information is different from and complementary to that obtained by optical microscopy, and can be achieved rapidly with only limited sample preparation.

As described in Chapter 5 optical microscopy study of polished epoxy embedded char particles enables classification into morphotypes based on an established classification system (Bailey et al., 1990; Rosenberg et al., 1996). In addition, it is possible to estimate macroporosity on the basis of optical microscopy (section 6.2.3). Such studies are, however, based on observations of particle cross sections and do therefore not describe surface structure and three dimensional form in detail. Such information is readily obtained by SEM.

With that in mind, 63 of the char samples obtained for the present project were investigated by SEM (Table 8.1). One of the early aims of the project was to develop a morphological classification based on SEM observations which could be correlated with the optical classification system. However, the latter is based on measurable observations of cross sections such as outer wall thickness and the size and number of pores. In contrast, SEM provides visual documentation of three dimensional form due to a great depth of focus, but not many quantifiable parameters which can be used for classification. A suggestion was made in a preliminary, unofficial report by Petersen, Guvad and Stouge (Optisk og SEM klassifikation af kokspartikler, 1994 (in Danish)), to classify char particles based mainly on their form, number of pores and, if visible, the existence of an internal network. However it is at the present stage not considered practically possible to correlate the two classification schemes with much certainty, mainly because the observations are of a complementary nature.

The performed SEM study has led to the preparation of an atlas of char particles formed from different coal types, by various technologies and at various temperatures and burnout (The Combustion Char Atlas, Sørensen and Rosenberg ,1996). The atlas will be published by GEUS both as a separate atlas and on CD-ROM. The CD-ROM media enables the user to examine images with maximum resolution and gives the opportunity to magnify specific details. A significant part of the following results and discussion are related to the Combustion Char Atlas. As will be discussed below the SEM study has yielded important information about the appearance and evolution of char microporosity as a function of burnout, features which are not readily visible by traditional microscopy.

8.2 *Analytical procedures*

Char particles were dispersed evenly on double stick conductive carbon tape mounted on an aluminium stub. The purpose of the coal tape is both to keep the particles in place and to conduct electric charge to the sample holder. A thin carbon coating was evaporated onto the powder sample to further facilitate conduction of electrons to prevent charge build-up during analysis.

The used scanning electron microscope is a Philips XL40 equipped with both an Everhart-Thornley secondary electron detector and a solid state backscatter electron detector. Both detectors were used in the present study. The images created by the secondary electron detector contain information about the topography and morphology of particles, whereas images created by the backscattered electron detector contain information of differences in average atomic number, i.e. the higher the average atomic number the brighter an appearance. This makes the backscatter images well suited to visualise the distribution and content of mineral matter because the minerals of interest are significantly higher in atomic mass than coal and carbonaceous material.

Four images are presented for each sample in the Combustion Char Atlas. Images were obtained at two magnifications - 150x and 300x respectively, and both secondary electron and backscatter images were taken at each magnification. This procedure was chosen to represent both details of the char morphology, as well as the distribution of pores and mineral matter. The fields illustrated in the Combustion Char Atlas were chosen to be representative of the prepared char samples. A field was chosen after examining a larger part of the char sample at low magnification, and scrutinising several areas at higher magnifications. It was found that different char types were relatively evenly distributed, and even though the field of view at 150x magnification measures only 0.6 mm by 0.8 mm, it was relatively easy to find fields which represent the general features of each sample illustrating the most common char types. Therefore it must be born in mind that char types which are rare in specific samples are not necessarily represented in the atlas.

Based on the acquired images and observations in Combustion Char Atlas, a number of additional images were obtained of selected particles at higher magnification. These images are presented in the following together with a number of images originating from Combustion Char Atlas.

8.3 Results

8.3.1 High and low temperature chars

As was indeed expected on the basis of the observations in Chapter 6 and Rosenberg et al.(1996), significant differences in the appearance of high and low temperature chars were noticed. Typical morphologies of low- and high-temperature chars at comparable burnout are shown in Figure 8.1. Low temperature chars formed in a drop tube furnace at Studsvik Energy AB are characterised by relatively large particles (up to 200μm) with elongated, spheroidal outlines (Figure 8.1a). Such particles are probably tenuispheres or crassispheres as defined in the classification proposed by Bailey et al. (1990). However it is usually not possible to look inside the particles unless they are broken and therefore, the agreement between the SEM image and the optical classification involves significant uncertainty.

High-temperature chars have typically more irregular outlines and often contain several macropores. Figure 8.1b shows an example which was formed in the laminar flow reactor at Sandia National Laboratories. The particles have a more angular appearance than the low temperature chars. The morphotypes of high temperature chars are difficult to asses by SEM , but the inspection of broken particles reveals their more massive nature with walls that are generally thicker than those of the low-temperature chars, and internal walls are usually present. High-temperature chars sampled from full scale experiments at Fynsværket have quite varied morphologies and are characterised by smaller grain-size than laboratory chars (Figure 8.1c and d). The smaller char particles are a result of the smaller particle size of the feed coals in the full scale experiments.

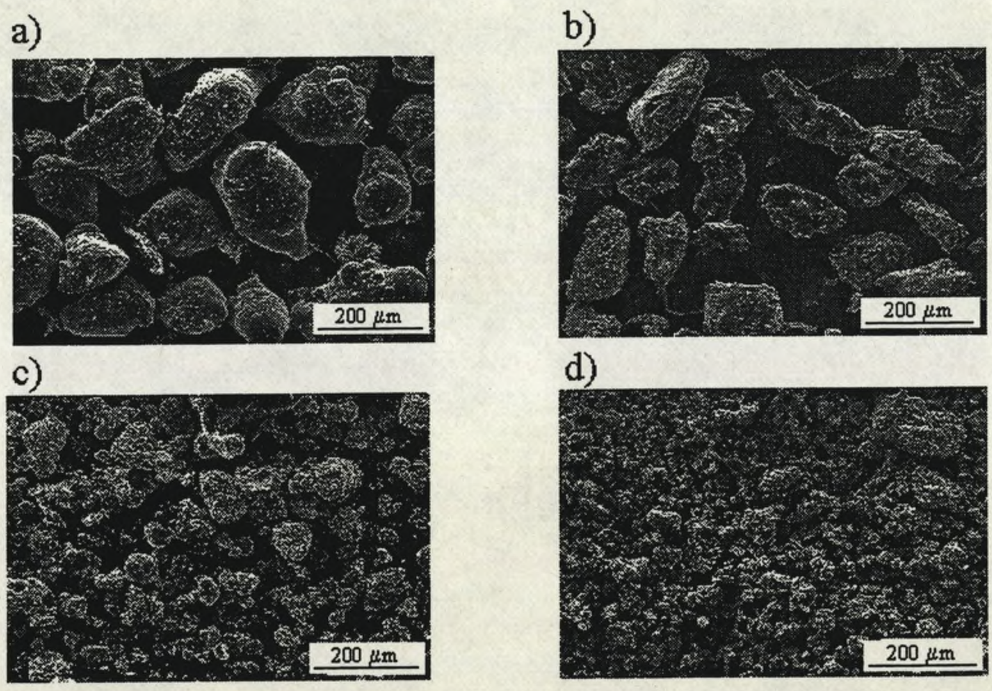

Figure 8.1 SEM photomicrographs showing typical char morphologies at similar burnout but produced at different temperatures. All images were obtained with SE detector. a) Low temperature char (CoD) produced in DTF at 800°C, burnout 53%. b) CoM, high temperature char produced in LFR at 1419°C, 12% oxygen, burnout 59%. d) CoP, full scale char from Fynsvaerket produced at c. 1500°C, burnout 63%. e) PoA, full scale char from Fynsvaerket produced at c. 1500°C, burnout 63%.

8.3.2 Mineral matter

The distribution of mineral matter on char particles is illustrated on backscatter images in the Combustion Char Atlas. Many of the mineral particles are located at the surface of chars, but no clear general correlation between mineral matter and char morphology is apparent. Comparison between Secondary Electron (SE) and Backscatter Electron (BSE) images reveals, however, that the "dusty" looking surfaces that are commonly observed on chars are composed mostly of a layer of mineral matter shining up brightly in BSE images (Figure 8.2).

a) b)

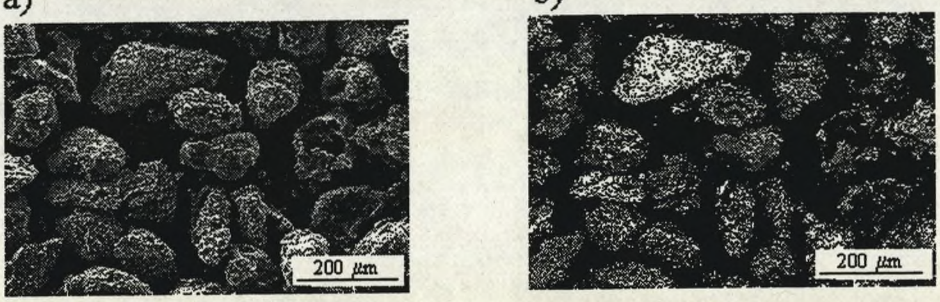

Figure 8.2 SEM photomicrographs of Au2M, Australian 2 coal derived char. Produced in LFR at 1593°C, 6% oxygen, burnout 58%. a) SE image showing surface morphology. b) BSE image showing mineral matter as light areas.

Theoretically, higher burnout level should be reflected in a higher proportion of mineral matter because burnout is estimated on the basis of ash content. In some cases it is possible to see such a correlation. An example is the progressive burnout sequence of Au2 char from 49% to 71% in 12% oxygen (Figure 8.3a-d). The proportion of mineral matter, appearing as light areas, clearly rise with increasing burnout. In other cases the correlation is lacking as for example in the burnout sequence from 59 to 84% of Co char in the presence of 12% oxygen (Figure 8.3e-h). The two most outburned samples in the latter case do not contain much mineral matter which is visible by SEM. A possible explanation is that the mineral matter is dispersed in the char structure instead of being concentrated in mineral grains. Such dispersed mineral matter will not reveal itself on a BSE image. A more detailed investigation of the relationship between mineral matter, its distribution on chars and its composition by SEM-EDX (energy dispersive X-ray analysis) would be of interest because mineral material may be important for char reactivity and effectivity of combustion (Menendez et al., 1994).

8.3.3 Microporosity

In Chapter 6 it was shown that macroporosity as measured by optical microscopy did not change significantly during burnout from around 50% to around 70%. The high resolution of SEM images gives the opportunity to estimate the variations qualitatively in both macroporosity and microporosity. In this context microporosity is defined tentatively as constituted by pores less than 5μm in diameter. Figure 8.4 shows SE images of chars formed from Au2 coal in the laminar flow reactor at Sandia National Laboratories in the presence of 12% oxygen. The burnout increases from Figures 8.4a to h. A striking feature associated with increasing burnout is a change in surface structure. At the lowest burnout level (Figure 8.4a and b) the surfaces are characterised by a relatively smooth appearance, several macropores and relatively few micropores. With progressive burnout particle surfaces become increasingly porous, ultimately ending up with very fragile appearing particles characterised by a multitude of micropores and diffuse grain boundaries (Figures 8.4g and h). No obvious accompanying change in the macroporosity was observed and was not noticed by optical microscopy (Chapter 6).

Figure 8.5 shows a similar evolution for char formed from Co coal under the same conditions as mentioned above. The burnout level ranges from 59% to 84%. An evolution similar to the one described for Au2 is apparent, i.e. particle surfaces change from having a relatively smooth appearance to being increasingly porous with ill-defined margins with higher burnout.

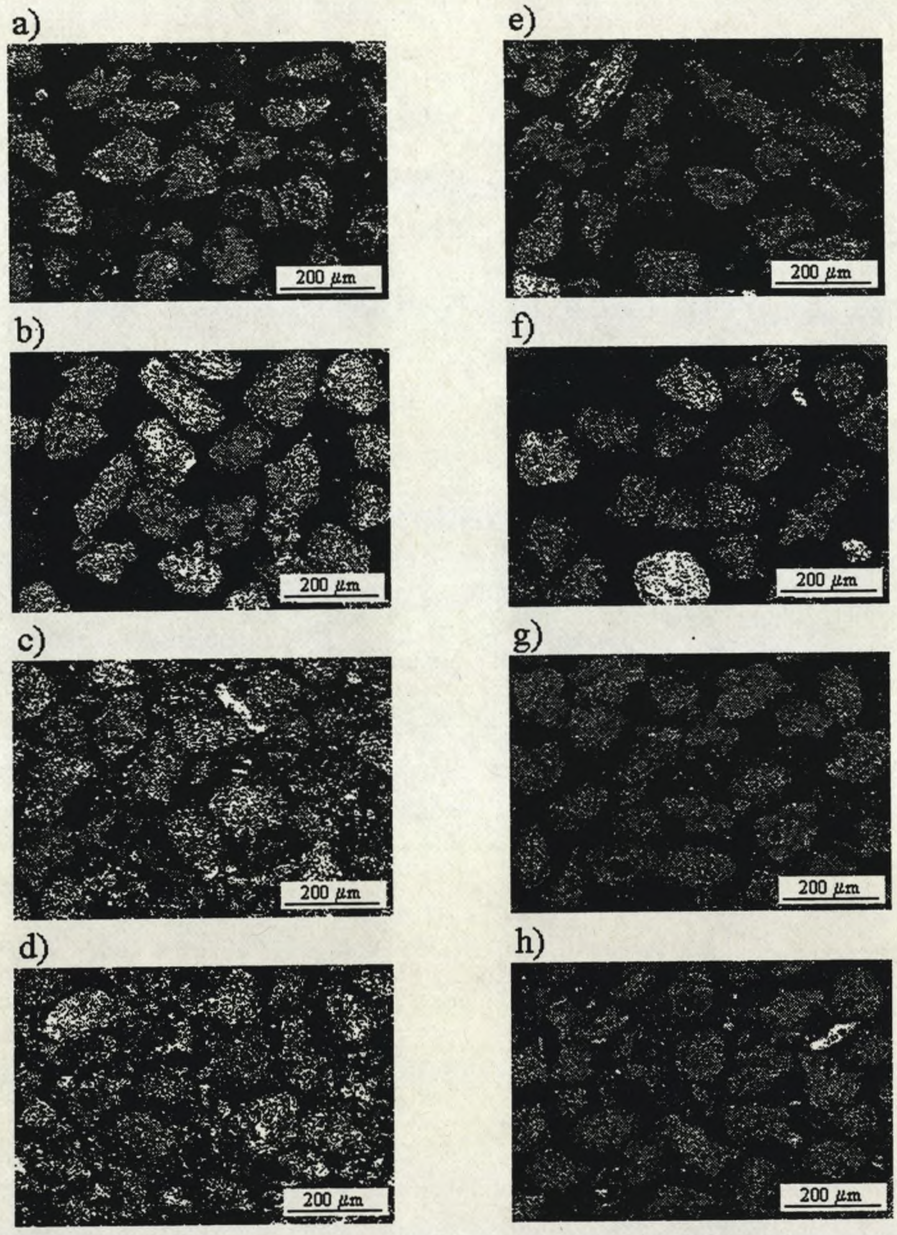

Figure 8.3 SEM photomicrographs showing BSE images. a-d) Au2O, Au2P, Au2Q, Au2R. Burnout increases from 49% to 71% through a to d. e-h) CoM, CoN, CoU, CoV. Burnout increases from 59% to 84% through e to h.

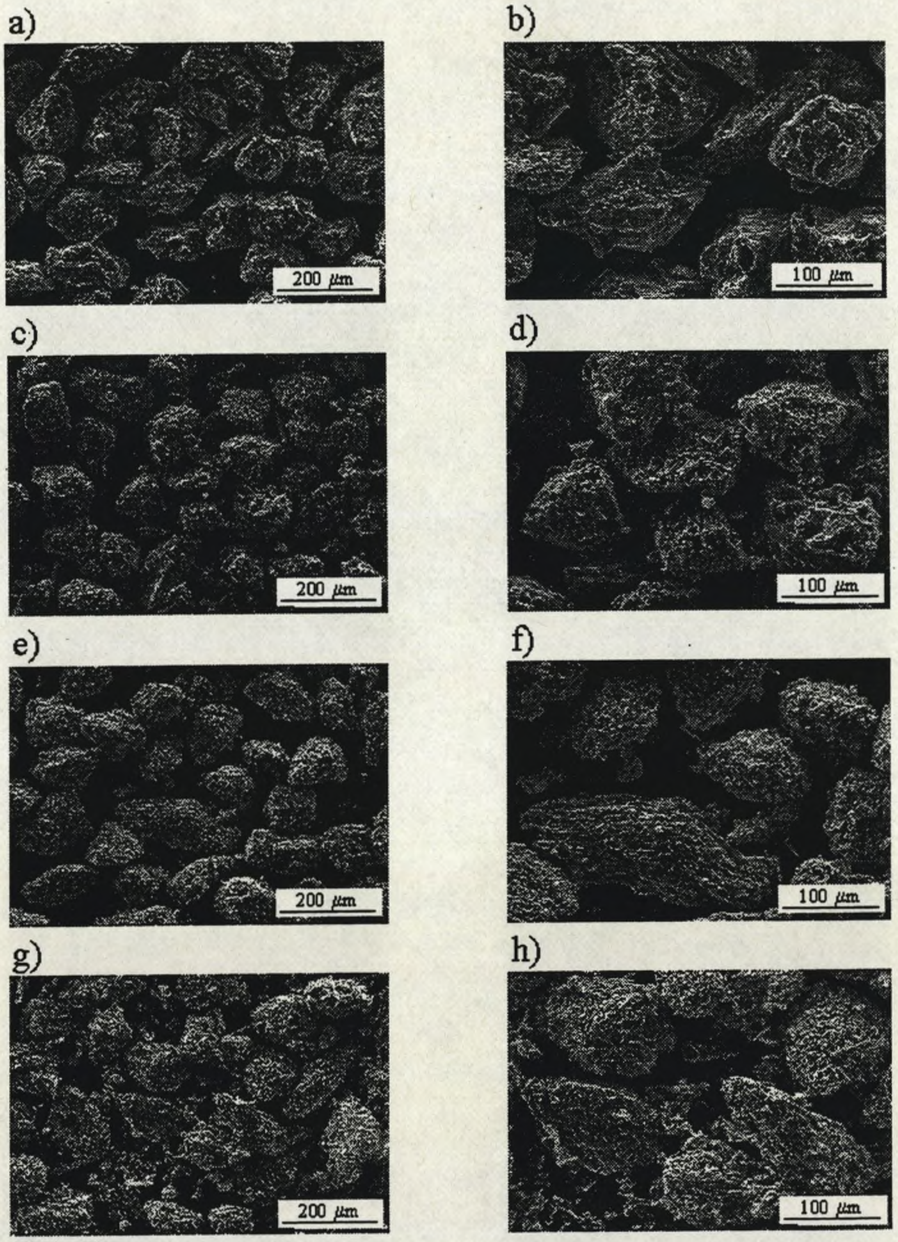

Figure 8.4 SEM photomicrographs showing morphological changes associated with increasing burnout for Australian 1 coal derived chars formed in LFR at 12% oxygen. Images were obtained at two magnifications (left and right column). a-b) Au1M, burnout 46%. c-d) Au1N, burnout 58%. e-f) Au1O, burnout 66%. g-h) Au1P, burnout 72%.

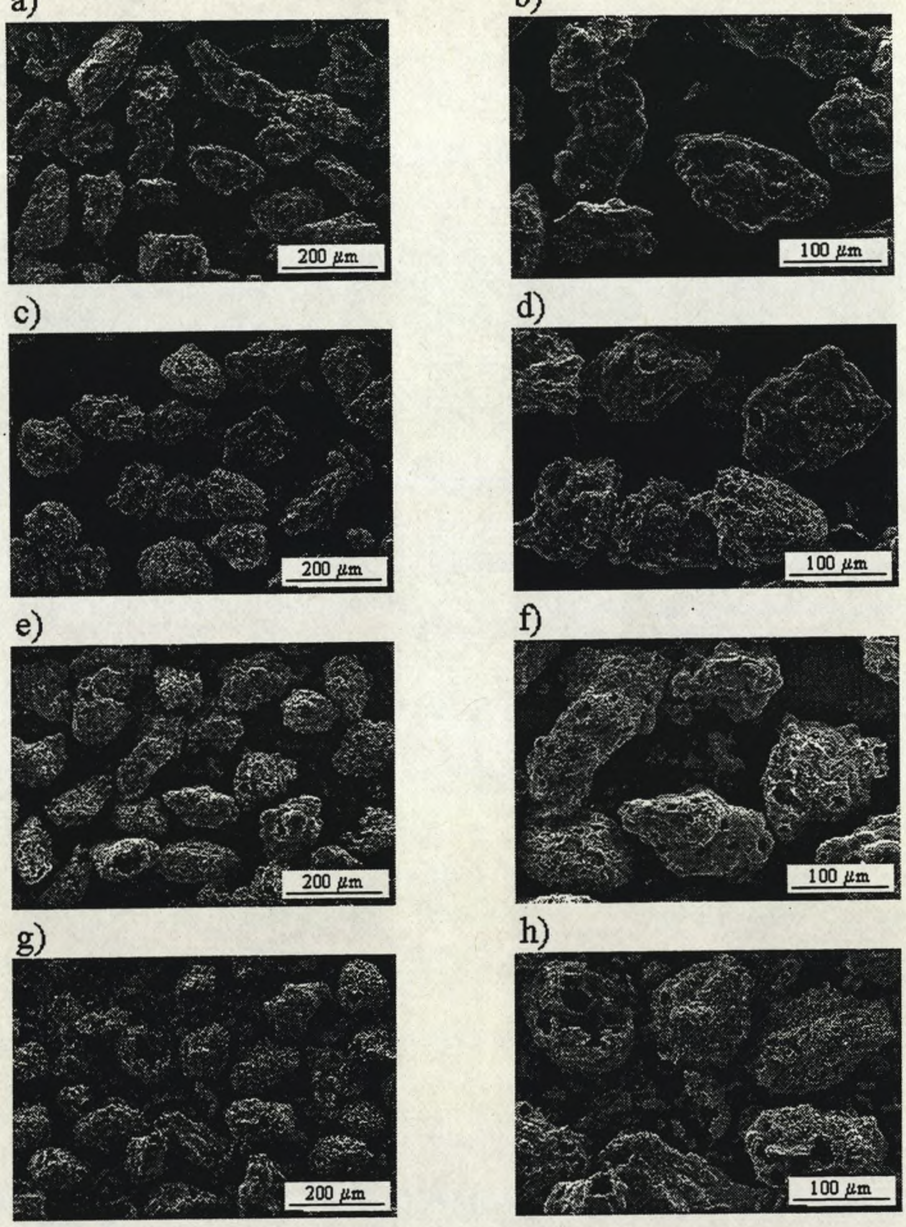

Figure 8.5 SEM photomicrographs showing morphological change associated with increasing burnout for Columbian coal derived chars formed in LFR at 12% oxygen. Images were obtained at two magnifications (left and right column). a-b) CoM, burnout 59%. c-d) CoN, burnout 70%. e-f) CoU, burnout 79%. g-h) CoV, burnout 84%.

These observations have led to a preliminary study of microporosity in relation to burnout for the experimental series of Au2 and Co in the LFR at 12% oxygen. To investigate the microporosity in detail a sequence of images were obtained at higher magnification (750x) (Figures 8.6 and 8.7). Broken particles were selected in order to study features such as internal structure and wall thickness of individual char particles. As seen in Figures 8.6a and b, Au2 char has a smooth outer surface with a low number of micropores at a burnout of 49%. The micropores appear to become larger across the wall-thickness towards the centre of the char. Internal walls contain a similar number of micropores. The outer wall has a thickness ranging from 3-8 μm (visual estimate).

At 62% burnout (Figures 8.6c and d) The Au2 char is equal in form to the one at 49%, but contains more micropores which are especially evident on the BSE image (Figure 8.6d). Mineral matter seems to be randomly distributed both on the surface and in the interior of the char. There is no clear difference in the number of pores at the surface and in the visible part of the centre.

At 66% burnout (Figures 8.6e and f) the Au2 char has larger and more micropores than observed at 62%, but is otherwise similar. It seems as if there is a tendency for mineral matter to be concentrated in clumps at the outside of the particle (Figure 8.6f).

At the highest burnout level of 72% (Figures 8.6g and h) he Au2 char is characterised by a multitude of pores that are significantly larger than the ones at 49% burnout. There is a clear tendency for mineral matter to be concentrated at the outer surface (Figure 8.6.h).

A burnout sequence from 59% to 84% of the Colombian char at 12% oxygen is illustrated in Figure 8.7. Figure 8.7a and b show a char particle at the lowest burnout level of 59%. As was the case for the Au2 chars at similar burnout, the surface is rather smooth with a few micropores. Also the inside of the wall contains small pores as well as "blisters" where gases were apparently exsolved but were unable to escape from the char structure.

Co char at 70% burnout (Figs 8.7c and d) has significantly more and larger pores than at 59% burnout. It appears as if the porosity is higher in the outer wall than in the interior walls. Probably many of the larger pores have been formed by coalescence of two or more micropores. Mineral matter seems to be confined mostly to the char surface (Figure 8.7d).

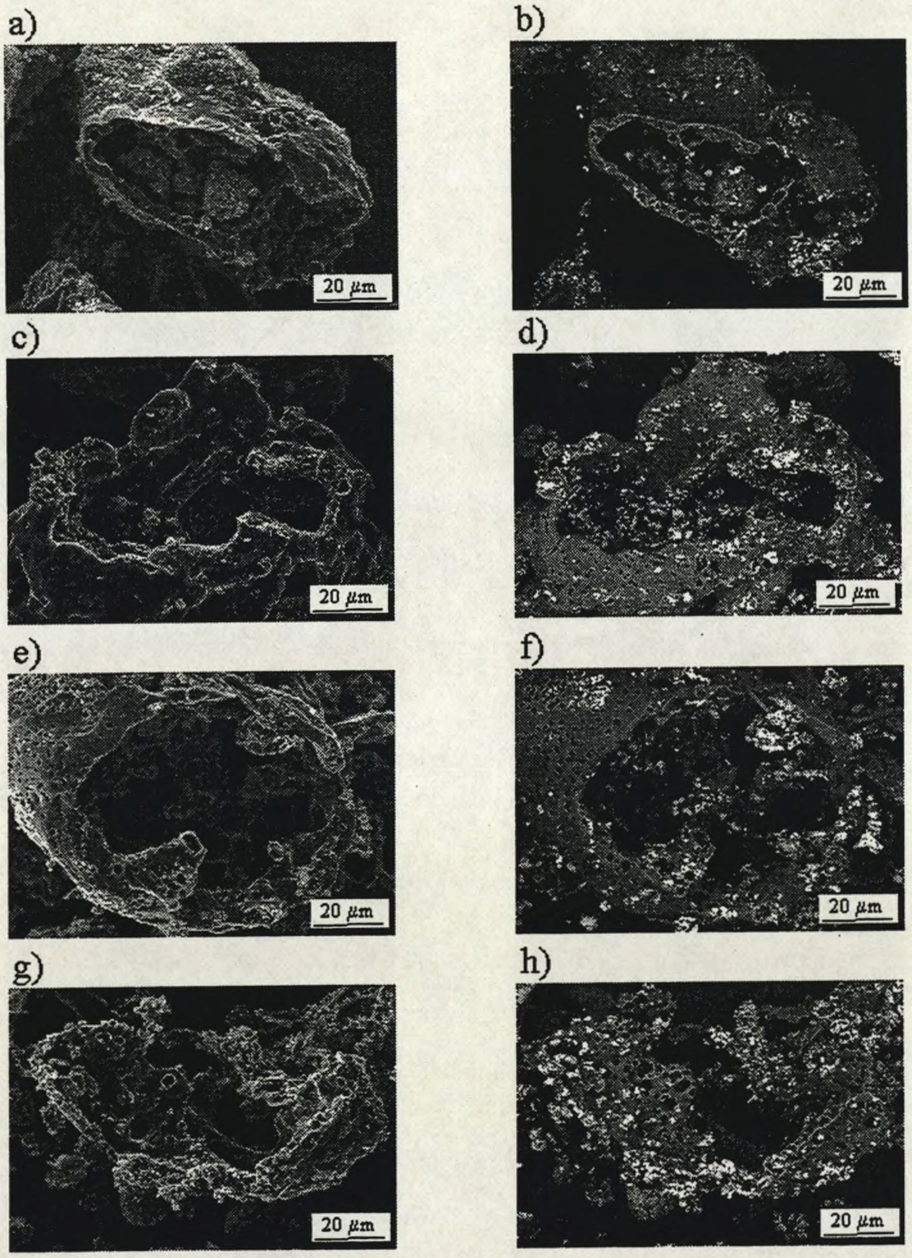

Figure 8.6 SEM photomicrographs showing broken chars in Australian 2 coal derived chars formed in LFR at 12% oxygen. Left column shows SE images and right column shows corresponding BSE images. Burnout increases downwards. a-b) Au2O. c-d) Au2P. e-f) Au2Q. g-h) Au2R.

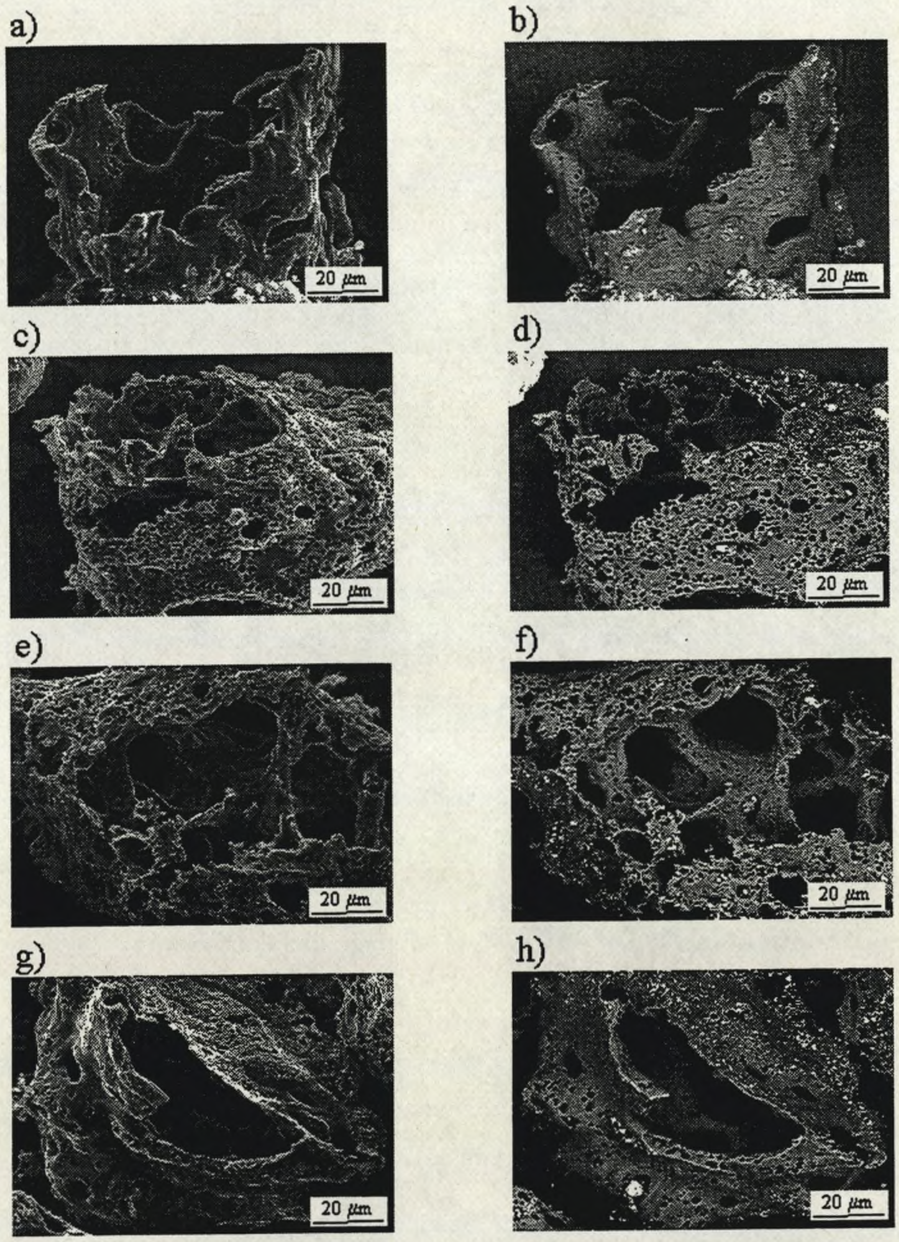

Figure 8.7 SEM photomicrographs illustrating broken chars in Columbian coal derived chars formed in LFR at 12% oxygen. Left column shows SE images and right column shows corresponding BSE images. Burnout increases downwards. a-b) CoM. c-d) CoN. e-f) CoU. g-h) CoV.

At 79% burnout (Figures 8.7e and f) Co char has a microporosity similar to the one at 70%. However, this particular particle has a higher macroporosity, but this is believed to be incidental (see below). The internal walls are also highly porous, but the pore size is slightly smaller than observed in the outer wall

At 84% burnout (Figures 8.7g and h) the wall of the illustrated Co char is highly porous with a number of pores ranging up to and above 5 μm. Many of these pores are probably formed by coalescence of micropores. Mineral matter seems to be confined mostly to the outside of the char (Figure 8.7h).

Evidently there are significant internal morphological variations between char particles within each sample in terms of both micro- and macroporosity. Nevertheless, the illustrations show the general trends which are accompanying progressive burnout: the macroporosity and the general morphology of particles do not change significantly during the burnout ranges studied here. However, both the outside and the interior walls exhibit drastic increases in microporosity with higher burnout level. In some instances it seems as if the microporosity is developed best in the outer wall, but this is not always the case. Generally mineral matter is concentrated on the outside of particles, but is also present in the interior of chars to some extent.

8.3.4 Relationship between char morphotype and evolution of microporosity

As mentioned previously it is difficult to establish morphotypes by SEM. It is, however, relatively easy to identify inertinite particles (inertoid and fusinoid) which appears as solid angular particles, occasionally with relict fusinite structure. A number of inertinite chars in highly outburned samples are shown in Figure 8.8. These images were obtained in order to asses whether inertinite chars behave differently from other chars in the present burnout range. Figure 8.8 reveals that inertinite did not develop microporosity to the same extent as the other char types.

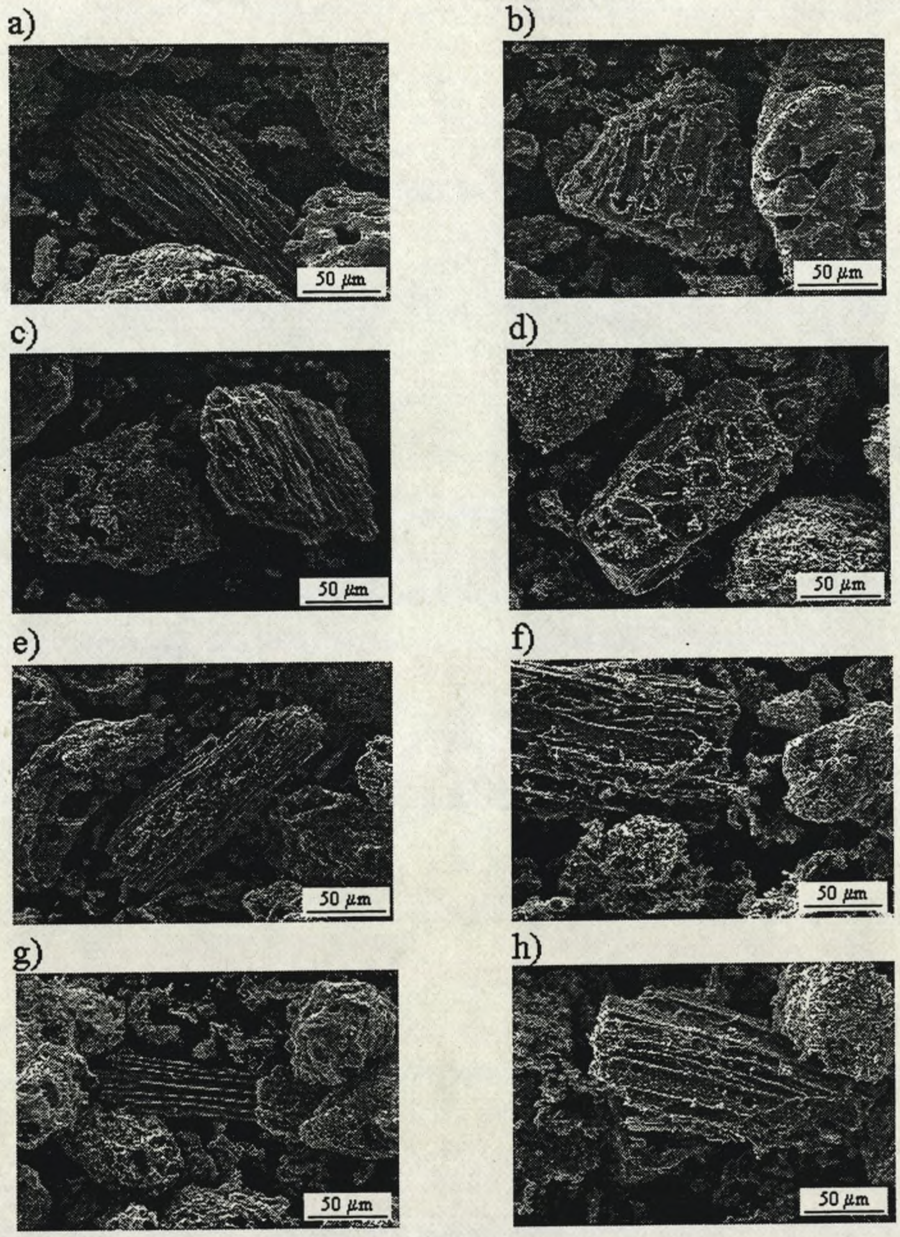

Figure 8.8 SEM photomicrographs illustrating solid inertinite type chars in high temperature chars at high burnuout. Some porous chars are also present in the images making it easy to see the minor development of microporosity in inertinite chars compared to that in porous chars. a-d) Inertinite chars in CoV, burnout 84%. e-f) Inertinite chars in Au1P, burnout 72%.

This suggests that inertinite and other char types behaves differently in the present burnout range. It was argued by Vleeskens et al. (1993) that the concentration of inertinite type chars does not change before about 98% burnout, i.e. until that point inertinite burn just as efficiently as porous chars. In this respect it is interesting that this preliminary study shows that their reactivity differs, as the microporosity develop more slowly on the inertinite derived chars than the porous chars. A more detailed SEM study of the structures of different char morphologies will be important to elucidate combustion behaviour and efficiency for different char types, features which are valuable in selection of coal types and combustion technique.

8.4 Discussion, conclusions and perspectives for future studies

The Combustion Char Atlas gives a useful reference material for char particle morphology, surface structure as well as macro- and microporosity. The chars illustrated in the atlas derive from different coal types and are at various burnout levels. They are formed in a variety of temperatures and by various experimental set-ups. Therefore, they cover a wide spectrum of the char types which future studies will encounter. Our hope is that comparison with Combustion Char Atlas will be useful in upcoming work on combustion.

The SEM images presented in this chapter has illustrated some of the changes which occur in char morphology in response to increased burnout, especially the development of microporosity which was not revealed by optical microscopy. In Chapter 6 it was shown that optically measured macroporosity did not change significantly in the studied burnout range, except perhaps for the Colombian derived chars at the final stage of the observed burnout. The SEM images suggest that this porosity increase may well be due to coalescence of micropores to larger and optically visible pores.

Inertinite type chars in this study did not develop as prominent a microporosity as other char types. This lends support to the notion that inertinite combusts differently than other chars. Together with the observations that the micropores develop at the outer as well as at the inner char walls, this supports the thesis that the char reactivity is highly dependent on the macroporosity and thereby the char morphology. More detailed SEM studies combined with optical microscopy and morphotype-classification would shed light on this aspect of combustion, which is important for combustion efficiency and therefore for economical performance at power plants.

A method for automatic measurement of total porosity (micro - and macroporosity) by SEM is under consideration at GEUS. The method involves automatic measurements of char area in polished cross sections and the total area of char particles including voids. The ratio between these two values can be used to estimate porosity. The advantage of SEM is its high resolution which enables the recognition of micropores. Char morphotype classification by SEM is, however, not a realistic possibility at present and is best achieved by competent optical microscopy study.

9 CONCLUSIONS

Systematic variations in the texture of chars produced in different temperature domains and heating rates have been demonstrated. These variations are found both using incident light microscopy on polished blocks and in SEM studies directly on the surfaces of the untreated particles. At temperatures above ~1300 °C and at heating rates similar to those in the commercial p.f. combustion boiler, it is possible in laboratory scale reactors to produce chars with similar morphology as those produced in a commercial p.f. combustion boiler. The results suggest that work in the field of char reactivity estimates and correlations between char morphology and coal petrography can be accomplished only on chars produced under temperatures and heating rates comparable to those for the intended use of the coal.

A general correlation between the coals' petrography and the morphology of high temperature chars has been found. A minor effect from the coals' rank may be observed, however, the number of coals studied is far to small to allow a statistical valid conclusion to be drawn. More work in the field of correlation between coal petrography and, in particular, the coal rank to char morphology needs to be done, by the inclusion of more coal types.

Generally it is found that the morphotype group crassinetwork/mixed network/mixed, is too complex and should be subdivided into smaller but more well defined groups.

The SEM study of the chars revealed extremely important information on the reactions after the devolatilisation stage has ceased. In the devolatilisation period the particles fuse, and the macroporosity and thus the morphotypes are formed. After the devolatilisation has ceased, secondary "micropores" are formed. The pores develop both in number and in size throughout the medium combustion interval. In this period no changes are observed with respect to macroporosity and morphology. In the end of the combustion interval the macrostructure breaks down, caused by coalescence of the increased number of micropores. This can be observed as a change in the macroporosity and in the morphology of the chars.

At this point the observations in the SEM are only qualitative. In order to make the method generally applicable, a quantitative characterisation method must be developed.

The results supports the thesis by Bailey et al. (1990), that the char reactivity is a function of the macroporosity and thus the morphology of the combustion chars.

10 ACKNOWLEDGEMENT

The authors wish to thank The Danish Energy Agency, Elsam I/S and Elkraft A.m.b.a. for their financial support and fruitful advises during the discussions at the steering meetings throughout the project. Dr. L. H. Sørensen, Research Centre Risø, is thanked for providing char samples from his laboratory scale experiments, and Karin Laursen for sampling full scale chars at Fynsværket. Finally Fynsværket is thanked for giving access to the full scale experiments.

11 REFERENCES

Bailey, J.G., Tate, A., Diessel, C.F.K. and Wall, T.F., 1990: A char morphology system with applications to coal combustion - Fuel, 69, 225-239.

Bend, S.L., Edwards, I.A.S. and Marsh, H., 1991: Coal provincialism, coal characterization and char formation - Fuel, 70, 1147-1150.

Crelling, J.C., Skorupska, N.M. and Marsh, H., 1988: Reactivity of coal macerals and lithotypes - Fuel, 67, 781-785.

Diessel, C.F.K., 1983: Carbonization reactions of inertinite macerals in Australian coals - Fuel, 62, 883-892.

Falcon, R.M.S. and Ham, A.J., 1988: The characteristics of Southern Africa coals - J. S. Afr. Min. Metall., 88(5), 145-161.

Gentzis, T. and Chambers, A., 1993: A microscopic study of the combustion residues of subbituminous and bituminous coals from Alberta, Canada - Int. J. Coal Geol., 24, 245-257.

Goodarzi, F. and Vleeskens, J.M., 1988: Reactivity of bituminous-semianthracitic coals: A reflected light study of their combustion residues (fly ash) - J. Coal Qual., 7(3), 80-85.

Hagelskamp, H.H.B. and Snyman, C.P., 1988: On the origin of low-reflecting inertinites in coals from the Highveld Coalfield, South Africa - Fuel, 67, 307-313.

Hardesty D.R., Pohl J.H. and Stark A.H., 1978: Sandia Report SAND78-8234, Sandia National Laboratories.

Hobday, D.K., 1987: Gondwana coal basins of Australia and South Africa: tectonic setting, depositional systems and resources. In: A.C. Scott (ed.), Coal and coal-bearing strata: Recent advances - Geol. Soc. London Spec. Publ., 32, 219-233.

Holland, M.J., Cadle, A.B., Pinheiro, R. and Falcon, R.M.S., 1989: Depositional environments and coal petrography of the Permian Karoo Sequence: Witbank Coalfield, South Africa - Int. J. Coal Geol., 11, 143-169.

Hunt, J.W., 1989: Permian coals of eastern Australia: geological control of petrographic variation - Int. J. Coal Geol., 12, 589-634.

Hunt, J.W. and Smyth, M., 1989: Origin of inertinite-rich coals of Australian cratonic basins - Int. J. Coal Geol., 11, 23-46.

Jensen, P.A., Rathman, O., Clausen, S., Andersen, S.A., Bech, N. and Kirkegaard, M., 1992: Final report Em. No. 1323/89-20, Risø-R-637, Research Centre Risø, Denmark.

Jensen, P.T. and Mitchell R.A., 1993: Energy Research Project no. 1323/87-16, subreport.

Jensen, P.T. and Thomsen E., 1990: Energy Research Project no. 1323/87-16, status report (in Danish).

Jones, R.B., McCourt, C.B., Morley, C. and King, K., 1985: Maceral and rank influences on the morphology of coal char - Fuel, 64, 1460-1467.

Kvalheim, O.M. and Karstang, T.V., 1987: A general-purpose program for multivariate data analysis - Chemometrics and Intelligent Laboratory Systems, 2, 235-237.

Laursen K. and Larsen O.H., November 1995: Slagging and Fouling, Full Scale Testing at Fynsværket Unit 7.

Martini, I.P. and Johnson, D.P., 1987: Cold-climate, fluvial to paralic coal-forming environments in the Permian Collinsville coal measures, Bowen Basin, Australia - Int. J. Coal Geol., 7, 365-388.

Menendez R., Alvarez D, Fuertes A.B., Hamburg G. and Vleeskens J., 1994: Effects of Clay Minerals on Char Texture and Combustion - Energy and Fuels, 8(5), 1007-1015.

Mitchell R.E., Hurt R.H., Baxter L.L. and Hardesty D.R., 1992: Sandia Report SAND92-8208, Sandia National Laboratories.

Rosenberg, P., Petersen, H.I. Thomsen, E., 1996: Combustion char morphology related to combustion temperature and coal petrography - accepted for publication, Fuel.

Stach, E., Mackowsky, M.-Th., Teichmüller, M., Taylor, G.H., Chandra, D. and Teichmüller, R., 1982: Stach's textbook of coal petrology - Gebrüder Borntraeger Berlin-Stuttgart, 535 pp.

Sørensen H.S. and Rosenberg P., 1996: Energy Research Project No. 1323/91-0012 and 1323/93-0018, Combustion Char Atlas.

Sørensen, L.H., Clausen, S., Asstrup, P., Jensen, P.A., Porsdal, H. and Olsen, A., 1991: Fundamentals in Combustion, Pyrolysis and Reactivity Measuremnets with a New Atmospheric Entrained Flow Reactor, and Description of a Burning Particle in a Controlled Atmosphere. Report. Section of Combustion, Research Centre Risø, Denmark.

Sørensen, L.H., 1994 : Fuel Reactivity as a Function of Temperature, Pressure and Conversion, Ph.D. Thesis, Reseach Centre Risø, Denmark.

Taylor, G.H., Liu, S.Y. and Diessel, C.F.K., 1989: The cold-climate origin of inertinite-rich Gondwana coals - Int. J. Coal Geol., 11, 1-22.

Thomas, C.G., Gosnell, M.E., Gawronski, E., Phong-Anant, D. and Shibaoka, M., 1993: The behaviour of inertinite macerals under pulverised fuel (p.f.) combustion conditions - Org. Geochem., 20(6), 779-788.

Thomsen E., 1993: ECSC Research Project 7220-EC/901, Combustion Reactivity of Coal Macerals. Final Report.

Thomsen E., Jensen P.T. and Rosenberg P., 1993: Energy Research Project No. 1323/87-16, Determination and Correlation of Coal Data, Final Report.

Unsworth, J.F., Barratt, D.J., Roberts, P.T., 1991: Coal Quality and Combustion Performance, part B, Coal Science and Technology 19, Elsevier.

Vleeskens, J.M., Menendez, R.M., Roos, C.M. and Thomas, C.G. 1993: Fuel Processing Technology , **36**, 91

Walker, S., 1993: Major coalfields of the world - IEA Coal Research 51, 130 pp.